GAZIANTEP UNIVERSITY
GRADUATE SCHOOL OF
NATURAL & APPLIED SCIENCES

PROPERTIES OF LIGHTWEIGHT AND NORMALWEIGHT CONCRETES WITH SIMILAR STRENGTH

M. SC. THESIS
IN
CIVIL ENGINEERING

BY
DILER SABAH ASAAD
DECEMBER 2011

Properties of Lightweight and Normalweight Concretes with Similar Strength

M.Sc. Thesis
in
Civil Engineering
University of Gaziantep

Supervisor
Assoc. Prof. Dr. Mehmet GESOĞLU

by
DILER SABAH ASAAD
December 2011

REPUBLIC OF TURKEY

UNIVERSITY OF GAZİANTEP

GRADUATE SCHOOL OF NATURAL & APPLIED SCIENCES

CIVIL ENGINEERING DEPARTMENT

Name of the thesis: properties of lightweight and normalweight concretes with similar strength

Name of the student: Diler Sabah Asaad

Exam date: 22/December/2011

Approval of the Graduate School of Natural and Applied Sciences

Prof. Dr. Ramazan KOÇ
Director

I certify that this thesis satisfies all the requirements as a thesis for the degree of Master of Science.

Assoc. Prof. Dr. Mustafa GÜNAL
Head of Department

This is to certify that we have read this thesis and that in our consensus/majority opinion it is fully adequate, in scope and quality, as a thesis for the degree of Master of Science.

Assoc. Prof. Dr. Mehmet GESOĞLU
Supervisor

Examining Committee Members	Signature
Assoc. Prof. Dr. Mehmet GESOĞLU	....
Assoc. Prof. Dr. Erhan GÜNEYİSİ	....
Assist. Prof. Dr. Ahmet ERKLİĞ	....

I hereby declare that all information in this document has been obtained and presented in accordance with academic rules and ethical conduct. I also declare that, as required by these rules and conduct, I have fully cited and referenced all material and results that are not original to this work.

Diler Asaad

ABSTRACT

PROPERTIES OF LIGHTWEIGHT AND NORMALWEIGHT CONCRETES WITH SIMILAR STRENGTH

ASAAD, Diler

M.Sc. in Civil Engineering

Supervisor: Assoc. Prof. Dr. Mehmet GESOĞLU

December 2011

90 Pages

This thesis addresses an experimental study conducted to investigate the performance of lightweight concrete (LWC) and normalweight concrete (NWC) with similar compressive strength. Lightweight concretes were produced with cold-bonded fly ash aggregates. For this, a dry powder mixture of 90% fly ash and 10% Portland cement by weight was pelletized through moistening in a revolving tilted pan at ambient temperature and cured for 28 days. A total of four concrete mixtures with designed compressive strengths of 25 and 45 MPa were developed for both LWC and NWC, namely LWC25, NWC25, LWC45 and NWC45. The concretes were tested at 28 and 56 days for water permeability, chloride ion permeability, gas permeability, and sorptivity index. On the other hand, compressive strength development of the concretes was observed at 7, 28, and 56 days. The results of comparing LWA with NWC indicated that the compressive strengths of both types of concrete for all ages were almost similar while water permeability of LWC generally slightly higher than that of NWC. Moreover, resistance to chloride penetration, gas permeability as well as sorptivity of LWCs was poorer than NWC.

Keywords:

Fly ash, chloride ingress, gas permeability, lightweight concrete, pelletization, water permeability.

ÖZ

BENZER BASINÇ DAYANIMLARINA SAHİP NORMAL VE HAFİF BETONLARIN ÖZELLİKLERİ

ASAAD, Diler

Yüksek Lisans Tezi, İnşaat Mühendisliği

Danışman: Doç. Dr. MEHMET GESOĞLU

Aralık 2011

90 Sayfa

Bu tez çalışmasında, benzer basınç dayanımlarına sahip hafif (LWC) ve normal betonların (NWC) performansları deneysel olarak araştırılmıştır. Hafif betonlar soğuk bağlama yöntemiyle üretilmiş olan uçucu kül hafif agregaları kullanılarak üretilmiştir. Hafif agregalar, eğimli dönerek çalışan peletleme diski içerisinde bulunan ağırlıkça %90 uçucu kül ve %10 portland çimentosu içeren kuru toz karışımın üzerine belirli miktarda suyun püskürtülmesiyle elde edilmiştir. Basınç dayanımları 25 MPa ve 45 MPa olan iki beton grubu tasarlanmıştır. Buna göre, 4 farklı beton elde edilmiştir (LWC25, LWC45, NWC25, NWC45). 28 ve 56 günlük kür süreleri sonunda, su geçirimlilikleri, klorür iyon geçirimlilikleri, gaz geçirimlilikleri ve kılcal su geçirimlilik katsayıları belirlenmiştir. Betonların basınç dayanımı gelişimleri ise 7, 28 ve 56 günlük test sonuçlarına göre belirlenmiştir. Betonların basınç dayanımı sonuçları bütün yaşlarda dayanım değerlerinin benzer olduklarını gösterirken hafif betonların su geçirimlilik değerleri normal betonlarınkine göre biraz daha yüksek olmuştur. Ayrıca hafif betonların klorür iyon direnci, gaz geçirimliliği ve kılcal su geçirimlilik değerleri bakımından normal betona göre daha düşük performanslı oldukları gözlemlenmiştir.

Anahtar kelimeler:

Uçucu kül, klorür geçirimliliği, gaz geçirimliliği, hafif beton, pelletization, su geçirmliliği

To my beloved parent,

brothers and sister

ACKNOWLEDGEMENTS

I would like to express my sincere gratitude to my supervisor Associated Prof. Dr. Mehmet GESOĞLU for his continual encouragement and supervision.

My honest respect to Assoc. Prof. Dr. Erhan GÜNEYİSİ, Prof. Dr. Ramazan KOÇ, Assist. Prof. Dr. Dlshad KAKASUR and Assist.Prof. Dr. Govand SHERWANI for his invaluable guidance, advices, without their support and contribution, this research project would not have been possible.

My special thanks are reserved for my parents, all my family, my daughter PRJA DILER, my wife GULER FAKHRADDIN; they have given me an endless enthusiasm and encouragement.

My sincere appreciation also extends to all my friends, Research Asst. Kasim MERMERDAŞ and Research Asst. H.Öznur ÖZ, those who were directly or indirectly involved in the process of producing this research report, for their generous assistance.

Finally, I would like to thank to those who took part in completion of this thesis.

TABLE OF CONTENTS

CONTENTS Page

LIST OF TABLES

LIST OF FIGURES

LIST OF FIGURES Page

LIST OF SYMBOLS/ ABREVIATIONS

ACAA	American coal ash association
ACV	Aggregate crushing value
C	Coulombs
CCP	Coal combustion product
CP	Coarse fineness
FA	Fly ash
FHWA	Federal highway administration
FP	Fine fineness
GGBFS	Ground granulated blast-furnace slag
GPOA	Ground palm oil fuel ash
HPC	High performance concrete
HPFC	High performance steel-fiber reinforced concrete
HVFA	High volume fly ash
IPC	Inorganic polymer concrete
K_a	Gas permeability
K_e	Water permeability
LWA	Lightweight aggregate
LWC	Lightweight concrete
MK	Metakaolin
NWA	Normal weight aggregate
NWC	Normal weight concrete
OFA	Original fly ash

OPC	Ordinary Portland cement
PFA	Pulverized fuel ash
RCC	Roller compacted concrete
RCPT	Rapid chloride permeability test
RHBA	Rice husk-bark ash
RPC	Reactive powder concrete
SEM	Scanning election microscopy
SP	Superplasticizer
VMA	Viscosity modifying admixtures
W/C	Water/cement ratio

PERSONAL INFORMATION

Name and Surname: Diler Asaad

Nationality: Iraqi

Birth place and date: Iraq-Erbil/01-January-1981

Marital status: married

Phone number: +90 539 645 9202

+964 750 499 9696

Fax: ------

Email: dilerasaad@yahoo.com

EDUCATION

	Graduate school	Year
Master ---------		
Bachelor	University of Salahaddin	2005
High School-------		

Work experience

	Place	Enrollment
2008-Present	Ministry of Higher Education	Civil Engineer
2006-2008	Ministry of Transportation	Civil Engineer

PUBLICATIONS

The paper (TRANSPORT PROPERTIES OF LIGHTWEIGHT AND NORMALWEIGHT CONCRETES OF SIMILAR COMPRESSIVE STRENGTH) was submitted to ACI materials journal and now under review.

FOREIGN LANGUAGE

English

Arabic

Kurdish

Turkish

HOBBIES

Studying

CHAPTER 1

INTRODUCTION

1.1 General

A rare credit of concrete that causes it really multipurpose is that it includes relatives of materials accompanied by a huge variety in density, strength and durability characteristics. Concretes of unit weight ranging from 1800-3000 kg $/m^3$ are practically used for structural purpose [1]. Current advancements in the construction of cement and workability improving substitutes have made it simple to fabrication of concretes with high compressive strength. Such concretes, however, are proportionately heavy with high weights. Moreover, NWC is made with natural aggregates. Clearly, these systems are seriously destructive to the environment. The other reasons for choosing lightweight concrete as a construction material is becoming increasingly important as more attention is being paid to energy conservation and to the use of waste materials to replace exhaustible natural sources. For example, the thermal resistance of such materials increases with decreasing the density which in turn leads to considerable energy savings [2]. Nevertheless, a concrete, including lightweight aggregate is simpler to mix and place than a normal weight concrete. In addition, Lightweight concretes (LWCs) in the strength range of 30–80 MPa can easily be made [1, 3]. Although Micro cracking at the interface will easily appear at early hydration due to higher absorption rate, pre-wetting the lightweight aggregate is one method of minimizing this effect and therefore, maintaining the consistency of the concrete mixes [4]. Approximately, there are 600 million tonns of Fly ash (FA) are available in the world, whereas only 10% of FA is currently [5]. Since big amounts of the fly ash stay unutilized in most countries of the earth, the creation of lightweight fly ash aggregates is a suitable step to greatly increase its use, especially, through the manufacturing of lightweight aggregate by the process, namely, cold bonding and sintering. It was possible to fabricate lightweight concrete with density in the range of 1560–1960 kg/m^3 and in the strength of medium range [5]. Expanding usage of LWCs brought the required for the production of artificial lightweight aggregates that possibly will be obtained by the cold-bonding process. Diversity of the sources and manufacturing processes for LWA necessitates better understanding of the influence of the lightweight aggregate characteristics on properties of the concrete [7, 8]. A more practical way of producing lightweight aggregate with an environmental impact and minimum energy consumption is the agglomeration of fly ash particles by cold-bonding process, where the water is the wetting agent acting as coagulant, so that the moist mixture would be pelletized in a tilted revolving pan [9, 10]. By using such aggregates, LWC with a compressive strength ranging from 20 to 50 MPa may be practically produced [8-11]. Some experimental studies have been conducted to explore how the aggregate type influences the properties of LWCs [12, 13]. It is reported that the compressive strength of LWCs is strongly affected by the material and binder type of LWAs [12, 14]. However, it is not clear if LWC strength has advantage over the NWC, strength of LWC can be improved substantially by the reduction of water/cement ratio (w/c) and by the incorporation of silica fume [11]. According to Khokhrin [15], the permeability of LWC manufactured through porous LWA is lower than that of NWC. It was referred to a combination of the improved interfacial zone between the aggregate and mortar matrix. Similarly, Thomas [16.] found that chloride penetrability of LWC made with blended cement and silica fume at a w/c of

0.30 were substantially lower than those of NWC. However, in the study of Al-Khaiat and Haque [13], concentration of chloride penetrated into the LWC was slightly higher than that in NWC of the same 28-day designed compressive strength of 50 MPa. As reported in the literature, the wide diversity of the lightweight aggregate source and manufacturing process result in distinctive behavior among the LWCs. Therefore, properties of LWCs should be investigate independently for each type of lightweight aggregate as far as the transport properties are concerned.

1.2 Research Significance

Lightweight concretes have certain properties which differs markedly those seen in normal weight concrete since there are many different types of LWA resource and production method which in turn result in distinctive behavior among the LWCs. Therefore, properties of LWCs should be investigated independently for each type of lightweight aggregate. For this purpose, an experimental study was conducted to investigate the transport properties of LWCs made with cold-bonded fly ash aggregates. Moreover, test results were compared to those of conventional concretes of similar 28-day design compressive strength. The performance characteristics of both lightweight concrete and the normalweight concretes were assessed in terms of compressive strength, water permeability, rapid chloride permeability, gas permeability and sorptivity.

1.3 Outline of the Thesis

Chapter 1-Introduction: Aim and objectives of the thesis are introduced.

Chapter 2-Literature Review and Background: A literature survey was conducted on the transport properties. The previous studies on the use of fly ash for producing lightweight aggregate are investigated.

Chapter 3-Experimental Study: Materials, mixtures, casting, curing conditions, and test methods are described.

Chapter4-Test Results and Discussions: Indication, evaluation, and discussion of test results are presented.

Chapter5-Conclusion: Conclusion of the thesis and recommendation for future studies are given.

CHAPTER 2

LITERATURE REVIEW AND BACKGROUND

2.1. Fly Ash

Fly ash is manufactured by coal-burning electric with moisture generating plants. Normally, ember is dried with played through air inside the steam boiler inflammation chamber wherever this immediately burns, giving rise to hotness as well as manufacturing a molten mineral. Steam boiler pipes draw out warmth as of the steam boiler, chilling the flue gas also leading to the molten mineral to stiffen and from ashes. Rough ash portions, applied to as bottom ash or slag, overthrow to the bottom of the inflammation chambers, while the slighter thin ash portions, called fly ash, continue postponed in the flue gas. Earlier to exhausting the flue gas, fly ash is discharged by particulate matter such like electrostatics precipitators otherwise filter material baghouses (Figure 2.1) [17].

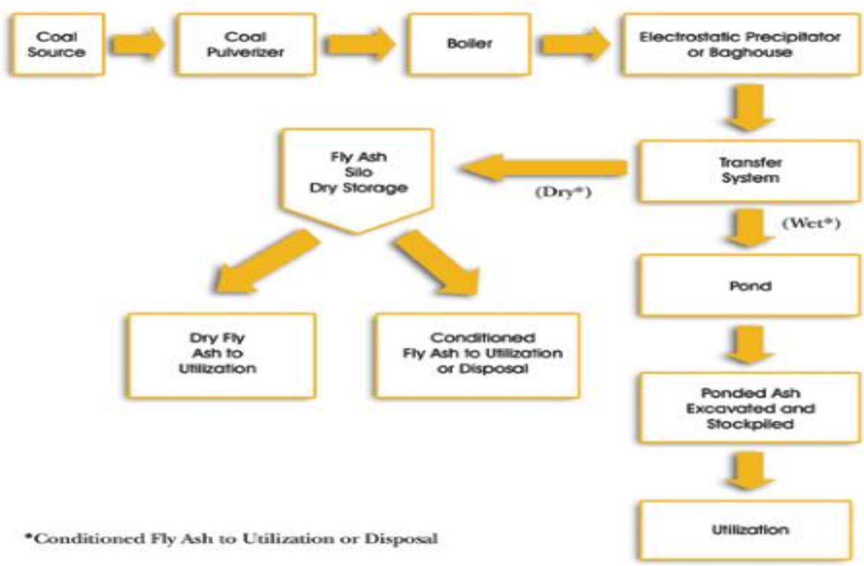

Figure 2.1 Method of fly ash transfer can be dry, wet, or both [17]

In previous, fly ash existed mostly published inside the air, however pollution control apparatus mandated in refreshed decades at the moment requires which being seized earlier to liberty. Fly ash is frequently maintained in thermal power plants or stored in nature. Almost, its 43 % is reused in U.S.A [18].

2.1.1. Mineralogical Properties of Fly Ash

Fly ash contains particles which are mostly ball shaped and in size in the middle 10 and 100 micron (Figure 2.2). The tiny glassware balls enhance the liquidity and fresh properties of concrete. Fineness is one of the important properties subscribing to the pozzolanic responsiveness of fly ash [17].

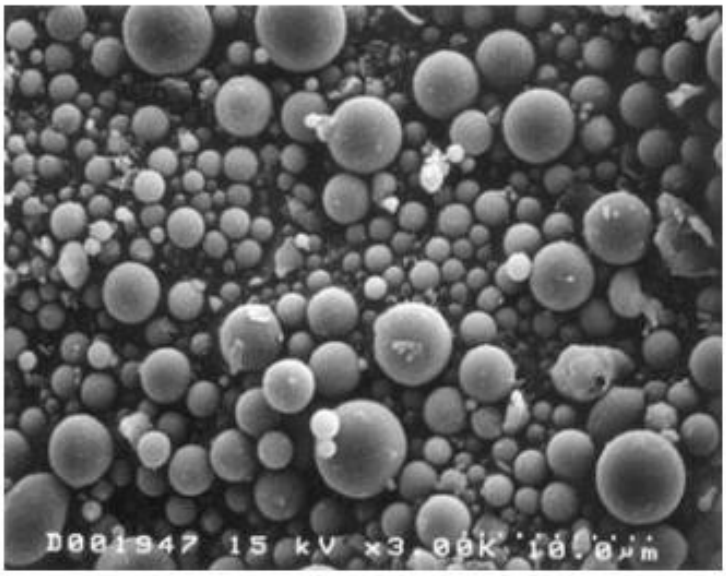

Figure 2.2 Fly ash particles at 2,000x magnification [17]

The coal constitution, combustion conditions, ash collection systems and other variables highly influence the constitution of the fly ashes. The constitution of fly ash is influenced by the rate of cooling. It is composed primarily (50-90 %) of mineral content in the form of the glassy particles [19, 20].

2.1.2. Chemical Properties

Fly ash coagulates while deferred in the emission gases as well as is collected by electrostatic precipitators or filter packs. As the fragments coagulate while deferred in the emission gases. They include mainly Of silicon dioxide, that is available in two forms: formless, that is circled and smooth, also crystalline, whatever is sharp, pointed and dangerous aluminum oxide and iron oxide. Fly ashes highly diverse, reaching of a mix of glassy particles with various recognizable crystalline stages such as quartz, mullite, and various iron oxides [21].

Two classes of fly ash are specified by ASTM C618 [22]: Class F and Class C fly ash. The main diversity among these classes is the quantity of calcium, silica, alumina and iron component in the ash. The chemical properties of fly ash are mostly affected by the chemical component of the coal burned. Class C ashes are usually received from sub bituminous coals and include principally of calcium alumino sulfate glasses, as well as quartzes, tricalcium aluminates, and free limes. Class C ashes are as well as related to as high calcium fly ash as it conventionally includes more than 20 % free lime.

Class F ashes are usually gained from bituminous and anthracite coal also consist primarily of an alumina-silicate glass, with quartz, mullite, and magnetite as well present. Class F, or low calcium fly ash has been smaller than 10 % free lime.

2.1.3. Physical Properties

Fly ash know how be tanned to be dark grey, relying on its chemicals and minerals element. Tan also brightness colours are typically connected accompanied by high lime component. A brown color is normally related with the iron component. A black gray to black color is normally referred to elevated unburned carbon component. Fly ash color is normally very regular with every power plant also coal informant [17].

Fineness of fly ash is the majority closely associated to the operating situation of the coal crushers and the grind ability of the coal itself. For fly ash use in concrete implementations, fineness is refined as the percent by weight of the material retained on the 0.044 mm sieve. A coarser gradation be capable consequence in a less reactive ash and could include higher carbon constituents. Limitations on fineness are reported by ASTM. Fly ash can be prepared by screening or air categorization to improve its fineness and reactivity. Some non-concrete implementations, such as constructional fills are not influenced by fly ash fineness. Nevertheless, another implementation such as asphalt filler is vastly relying on the flyash fineness and its particle size distribution [17, 24].

Figure 2.3 Typical ash colors [17]

2.1.4. Utilization Areas of Fly Ash

In U.S.A, 2006, nearly 32.4 million tonns of fly ash were utilized [26]. These are nearly a 5 % increase in the usage of fly ash over the past year. The greater part of this utilization can be applied to the production of concrete and grout. Figure 2.4 displays the 2006 percentages of fly ash utilization for common construction implementations.

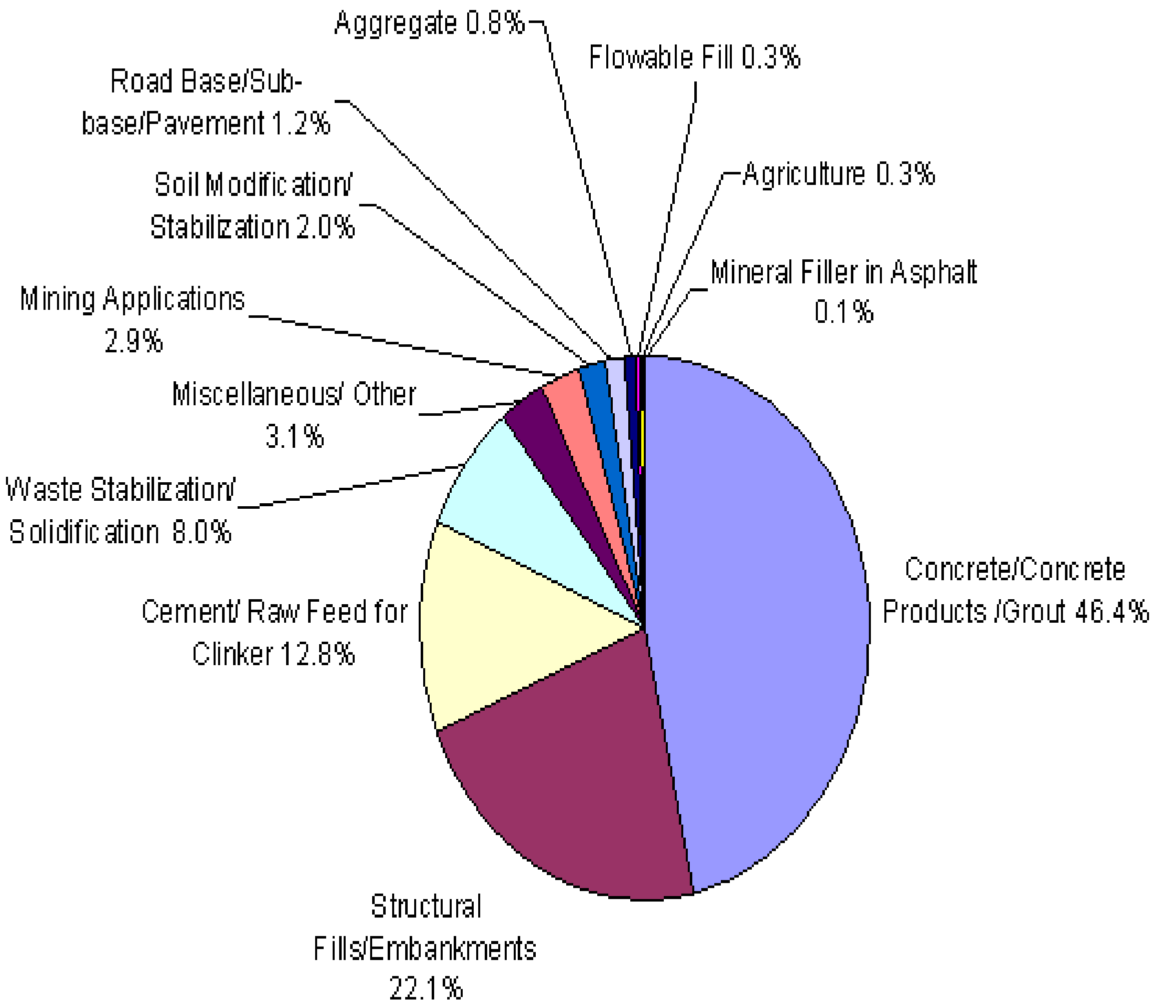

Figure 2.4 Common applications of fly ash [26]

Fly ash is applicable in various implementations because it is a pozzolan, meaning it is a siliceous or alumina-siliceous material that, whenever in a finely divided from also in the attendance of water, will incorporate with calcium hydroxide to form cementitious compounds [27].

2.2. Lightweight Aggregates (LWA)

Lightweight aggregates are naturally found or the others are manufactured. It is a granular material with a bulk density not exceeding 1200 kg/m^3 or with a particle density not exceeding 2000 kg/m^3 [28].

2.2.1. Natural Lightweight Aggregate

The best known of natural LWA are pumice, scoria, volcanic cinders, tuff, and diatomite and the most widely used are pumice and scoria. Aggregates are produced by mechanical handling of lava (crushing, sieving and grading). Pumice is produced when the molten SiO_2 which lava from the explosive eruption of a volcano cools. Sudden cooling freezes the material existing at molten state. The presence of gas bubbles in the molten lava makes low density of the pumice which becomes trapped on cooling. Its dry bulk density ranges from 5 to 9 kN/m^3 DiatFomite is a silicious sedimentary rock, whatever includes primarily of fossilized skeletal remains of diatoms. It is usually established in volcanic environments, accompanied by the deposits shaping in lakes in volcanically active areas. It is very finely permeable also very low in density [29, 30].

2.2.2. Artificial Aggregate from Industrial by Products

2.2.2.1. Furnace Clinker

The construction of clinker is by-product of the combustion of coal in domestic or industrial firing systems. It is used as lightweight aggregates, after crushing and screening, which is dark color, hard and with a sintered or slaggy appearance. This type of aggregate is used mostly in the manufacture of concrete blocks. In addition, it is not advised for producing concrete because of containing sulphates and chlorides [31].

2.2.2.2. Foamed Slag

There are two main kinds of slag: blast furnace slag in addition to steel furnace slag. Blast furnace slag is a side-effect from the melting of iron ore otherwise iron little balls through coke and a flux, such as limestone or dolomite. The calcium in the stone mixes with the aluminates and silicates in the ore also ash from the coke to manufacture this nonmetallic material. The slag is removed from the furnace for furthermore preparing. Blast furnace slag be capable be used in the fabrication of clinker, blended cementsand as an aggregate in cement concrete. Steel slag is a secondary product since the processing of iron or scrap steel in a necessary oxygen furnace otherwise electric arc furnace. Over again limestone or dolomite is used as a flux to take off infections. The steel furnace slag is air chilled, and after free iron, results are taken off, it be capable be used as a raw material in the fabrication of clinker. For 2003, the United States Geographical Survey assessed that 8.8 million metric tonnsof steel furnace slags were manufactured, and that over 5% of it was used by cement plants to manufacture clinker [32].

Figure 2.5 Slags [32]

2.2.2.3. Bottom Ash Lightweight Aggregate

Coal combustion bottom ash can be similar in many ways to manufacture aggregate. The high temperatures during combustion in combination with turbulent air flow results in a porous bottom ash with bulk densities of 45 to 75 Ib/ft^3, similar to manufactured aggregate. Adequate processing of the bottom ash can potentially provide the gradation that would enable the use of this material as a lightweight aggregate [33].

Figure 2.6 Bottom Ash [34]

2.2.3. Industrially Produced Artificial Lightweight Aggregate

Investigators have advanced techniques for producing artificial LWAs in factories from the natural raw materials like expanded clay, shale, slate, etc., as well as from industrial by products such as fly ash, bed ash and blast furnace slag.

2.2.3.1. Leca and Fibo

Leca (produced in the UK) and Fibo (produced in Scandinavia) are expanded clay aggregates produced in a rotary kiln that consists of a long large-diameter steel cylinder inclined at an angle of about 5° to the horizontal. The kiln is lined internally in the Firing zone with refractory bricks whatever as the kiln rotates become heated to the required temperature and 'roast' the clay pellets for the required degree of expansion to occur. The length and formation of the kiln depend in part on the composition of the clay and length of time. It takes to 'condition' the clay pellet in the pre-heater to obtain a temperature of about 650°C to avoid it shattering before becoming pyroplastic.

Throughout the progress of the prepared material through the kiln, the temperature of the clay pellets progressively rises up to the time of expansion actually occurs. The expanded product is discharged from the firing zone as soon as possible for cooling to freeze the particles at the wished degree of expansion. Cooling possesses place either in a rotary cooler or fluidised bed heat-exchanger. The finished product is graded, and if it's necessary crushed to particle sizes less than 16mm, while the particle density can be varied relying on the range of temperatures at which expansion takes place [35, 36].

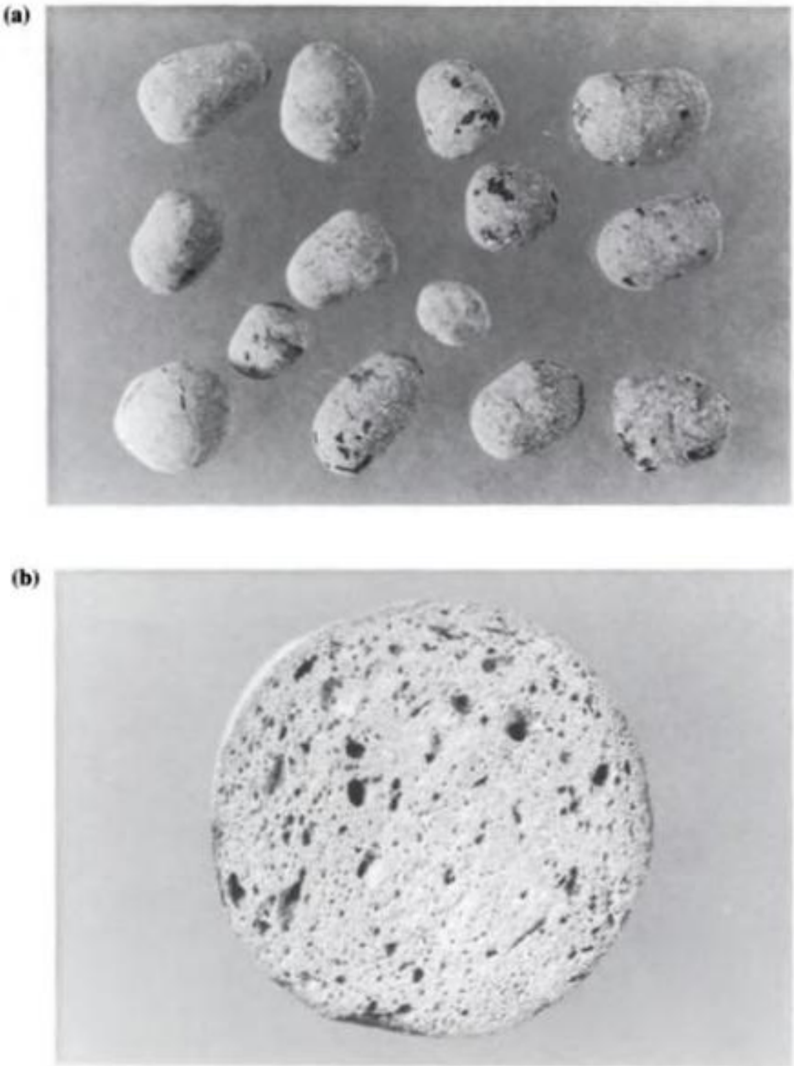

Figure 2.7 (a) Typical Leca particles, 12mm size. (b) Sectioned Leca particle about 30x enlarged. [35]

2.2.3.2. Perlite

The categorizing point that sets perlite aside as of other volcanic glasses is that whenever heated to suitable point in its softening scope, it widens starting 4 to 20 times its primary volume. This development is due to the occupancy of 2 to 6 % merged water in the crude perlite rock. When rapidly heated to above 871°C, the crude rock pops in a mode like to popcorn as the merged water evaporates also formulates endless little bubbles, whatever account for the huge lightweight and additional abnormal physical properties of widened perlite. This expansion

Process as well as composes one of perlite's most categorizing characteristics: its white color. Crude stone possibly will variety starting transparent light gray to glossy black, the color of widened perlite varieties as of snowy white to greyish white. Perlite is excavated and widened all over the globe. The United States is assessed to be the biggest user and manufacturer of crude and widened perlite. Another lead nation manufacturing perlite includes China, Greece, Japan, Hungary, Italy, Mexico, Philippines, and Turkey [37].

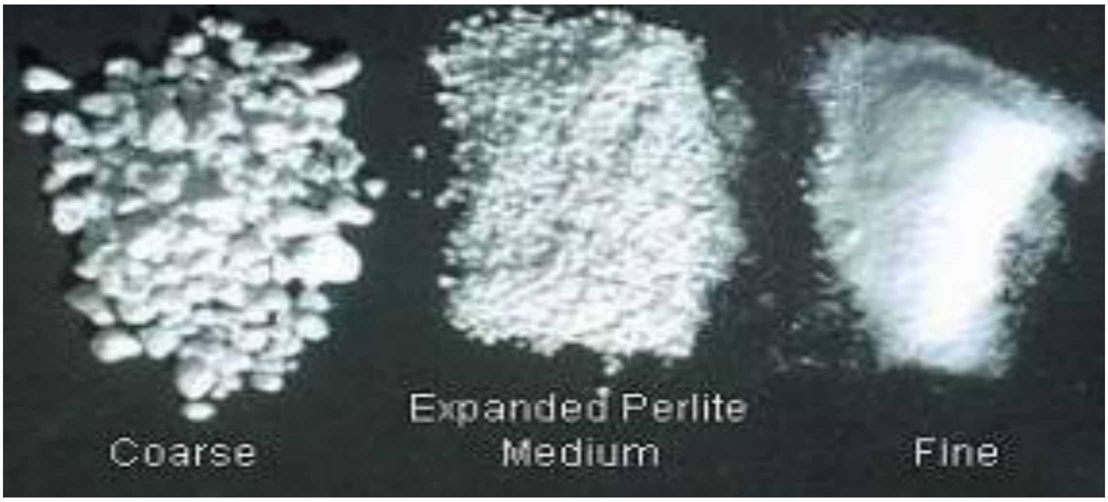

Figure 2.8 Perlite [37]

2.2.3.3. Vermiculite

Vermiculite is a natural mineral that widens with the implementation of heat. The enlargement procedure is named as exfoliation, as well as it is trading accomplished in purpose designed commercial furnaces. Vermiculite is shaped by weathering or hydrothermal transposition of biotite or phlogopite. This conventionally occurs as an alteration product at the connection between Accompanying and mafic or ultramafic rocks such as pyroxenites and dunites. It also happens in carbonatites and metamorphosed magnesium rich limestone. Associated mineral phases include:

corundum, apatite, serpentine and talc it occurs interlayered with chlorite, biotite and phlogopite [38].

2.2.3.4. Vegetable Aggregates

Some of the vegetable materials can be used to give stable, non-destructive, waterproofing, non-combustible aggregates. Examples are the wood aggregates, rice balls and cork aggregates. Wood aggregates are used to produce lightweight concrete, especially for soundproofing applications. There are a number of physical and chemical interactions between wood and cement, which can delay cement hydration. That’s why, a thermal treatment and a mineralization of wood aggregates are often essential before they can be used.

2.2.3.5. Slag Pellet

At first, the process was developed in Canada. Slag pellets are produced from the molten slag coming from furnaces by various injections of water followed by a mechanical dispersion with a rotary dram. An internal expansion is provided by the injected water which gives a steam vapor. Then shaped pellets are quickly cooled in the air, and vitreous external shell is created. The pellets fall back on an inclined ground covered with grates in a way that the greater particles are projected far away while the smaller ones fall nearer. In order to remove the water the pellets are heated [39].

2.2.4. Lightweight Aggregate Production with Fly Ash

Only a few amounts of fly ash are utilized in the worldwide. The main aim using fly ash for lightweight aggregate production is a feasible way for recycling of waste materials. Manufacturing fly ash lightweight aggregates can be achieved by sintering or cold-bonding methods.

2.2.4.1. Sintering Method

Artificial lightweight fly ash aggregates are manufactured using sinter strand; fly ash with clay is mixed with water and pelletized. The pellets are instantly subjected to a temperature of approximately 1100°C in the ignition chamber which uses reprocessed oil to fire the carbon in the pellets. The pellets are gone through the process of drying, grinding, sintering and cooling, ending up with a fly ash lightweight aggregate. At the end of the strand, the final pellets are naturally or mechanically separated. Then the material which is less than 2.5 mm is pulled off, after passing over a primary screen. For secondary screening, material above 2.5 mm is transferred through the conveyor to the required sizes for the appropriate market [36, 39].

2.2.4.2. Cold Bonding

Is a procedure wherever lime or cement is supplemented to fly ash, along with other materials like limestone, clay or shale. The main manufacturing process of fly ash lightweight aggregate consists of pelletizing and curing.

2.3. Pelletization Process

2.3.1. Definition of the Pelletization Process

Is a process for manufacturing pellets, a ball like shape of ash made by agglomeration of humidified fines in a revolving named drum. Binder addition possibly will as well as made to the fines throughout or prior to procedure. The goods at the finalization of the procedure is named as "the fresh pellet”. It may as well be sintered through a specified interval of time afterwards production relying on few concerns. The idea of pelletization process was first place forward by A. G. Anderson, a Swedish researcher, in 1912, and then by C. A. Brackelsberg in Germany, who planned a similar balling process was a revised process with the addition of binder to the fines agglomerated, and the pellets strengthened at elevated temperatures for the time of production. Studiers on pelletization process started in United States in 1920 due to demand of sintering concentrates that were used in Taconite- ore dressing procedure [20, 40].

2.3.2. Theory of Pelletization

Whenever a fine grained material is humidified, they form a slim moisture film on the skin of the fragments, whatever shapes a semilunar cartilage between the fragments, structure like bridges (Figure 2.9 a). In a situation, the fragments are revolved in a balling drum, then there forms sphere form structures accompanied by enhanced bonding forces between fragments due to centrifugal and gravitated forces (Figure 2.9 b and c). In pelletization process, the force advanced on the pellets expels the air that fills the free gap between the individual fragments, exiting the voids to fragments also water. As the fragments take closer, the structure comes to be denser, whatever enhances the structure consistency and causes the fresh pellets to possess adequate intensity for handling and accumulating conditions [41].

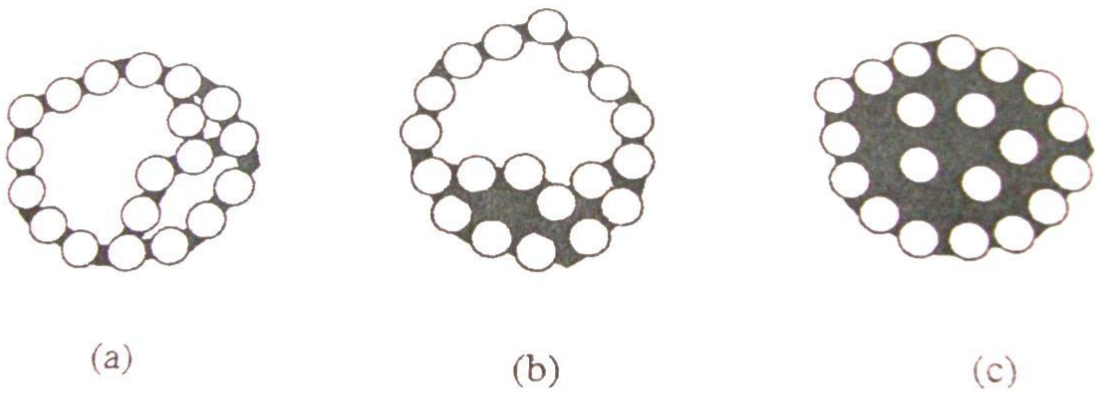

Figure 2.9 Mechanism of pellet formation [40]

The maximum strength of pellets may just be attained if all the capillaries are filled by water for the time of manufacture. The lack of adequate water reasons aired voids to be entrapped inside the structure, which controls the capillary activity. For fly ash, the ideal water content should be in the middle 20 and 25%. The granulometric distribution of the pelletized material is as well as excessive significance. The granulometric distribution of pellets may be restrained for the time of pelletization procedure by checking the feeding ratio of the binder and water content. The mechanism of sphere creation for the moisture content is less than the ideal state (Figure 2.10). In this condition, the moisture fragments move closer as well as come to be joined with water bridges. While in Figure 2.11, the mechanism of sphere creation is shown through moisture content above optimum. In this state, the formation is weaker and the capillary force is diminished because of wetting excessively. The formations are random sized and may be easily destroyed by the mechanical forces created in the balling drum and disc [20, 39, 40, 41].

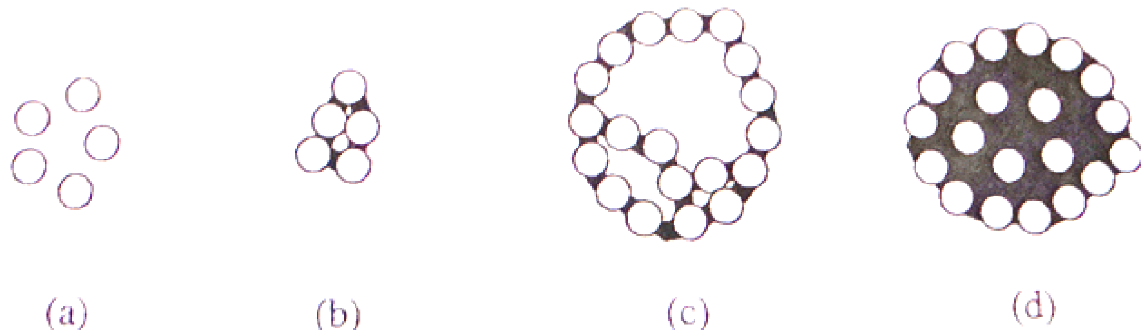

Figure 2.10 Mechanism of ball nuclei formation (water content below optimum state) [40]

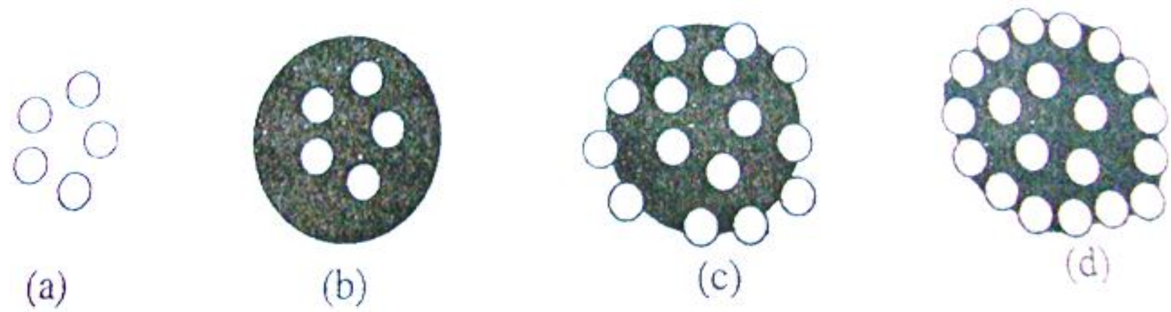

Figure 2.11 Mechanism of ball nuclei formation (water content above optimum state) [40]

2.4. Transport Properties of NWC and LWC

2.4.1. Transport Properties of NWC

It is well known that transport properties directly have the majority significant factor restraining the durability of cement based composites [42, 43]. Deterioration due to chloride ions from de-icing salts or seawater is resulted in the transportation of a chloride solution into the material.

There are two engines controlling the uptake and transportation. Permeability, which is a measure of the flow under pressure in a saturated porous medium, and sorptivity, which characterizes the material's ability to absorb and transfer water through it by capillary sucking [44]. The transport properties of concrete rely on principally on the number, size also distribution of pores in the cement paste and the aggregates. The air pores may be empty or water filled, relying on exposure former times the concrete, and this has an important effect on calculated transport properties [45]. Wong et al. [46] found that the drying raises the accessible transport paths and then the transport rates, for example, for the denser specimens of w/c of 0.35. Considering the one year aged specimens as an example, draining from75% r.h. to 50 °C increases the diffusivity, sorptivity and permeability on average at a factor of 13 for the w/c of 0.35 specimens, and a factor of 3.5 for the w/c of 0.5 samples, and they investigate that air entrainment raises gaseous diffusivity also permeability by up to a factor of 2–3 at the highest air contents, even so, of the w/c ratio, curing period as well as the conditioning regime. Heede et al. [47] noted that in addition to total porosity, pore connectivity and size are equally important for the transport properties of concrete. In all cases, porosity is linked to the degree of continuity of the pore system, which significantly affects the transport properties of concrete [48].

2.4.2. Transport Properties of LWC

Concrete transport properties are controlled by the transport properties of its constituent phases and their geometric arrangement [49]. For NWC, the aggregate commonly used in concrete has much lower transport properties than cement paste. While this difference in LWC, are so small or nearly equal. The main characteristic of the matrix structure of concrete that relates to the transport mechanisms are the pore system of the cement paste [44]. NWA contain pores which are discontinuous and do not allow water movement by capillarity, However, despite the higher porosity at the LWA, it is generally found that water movement in LWC is higher. The transport through concrete due to a pressure gradient depends largely on the inherent microcracking within the concrete and the interconnected pore network [42, 50]. The gaseous transport and water absorption happen just through empty pores and cracks. A decrease in transport properties with reduction in w/c ratio. For example, the w/c 0.35 samples would have a finer pore structure compared to the w/c 0.50 samples, so that for a given conditioning relative humidity, a larger fraction of pore structure remains water-filled due to capillary condensation [46].

The spatial arrangement of the air voids at a given air content relies on the size distribution of the voids. Wong et al. [46] used a simple formulation using Maxwell's model and predicted that an increase of 1% air content leads to increase the penetration coefficient by almost 10% or a 4 % reduction in it, depending mainly on the role of the air voids whether they behave as conductors or insulators. Little work has been directed to clarify the effect of using fly ash light weight aggregate concrete on the transport property.

2.5. Tests for Transport Properties

2.5.1 Water Permeability Test

Tam et al. [51] investigated that the typical permeability coefficient of Reactive powder concrete (RPC) at around 98 days is about 0.0005 also they investigated that low water penetration of Reactive powder concrete with low w/c may be attributed to tiny and disconnected pores which is available in the very homogenous, and dense paste of RPC. The relation between water permeability and w/b are shown in Figure 2.12.

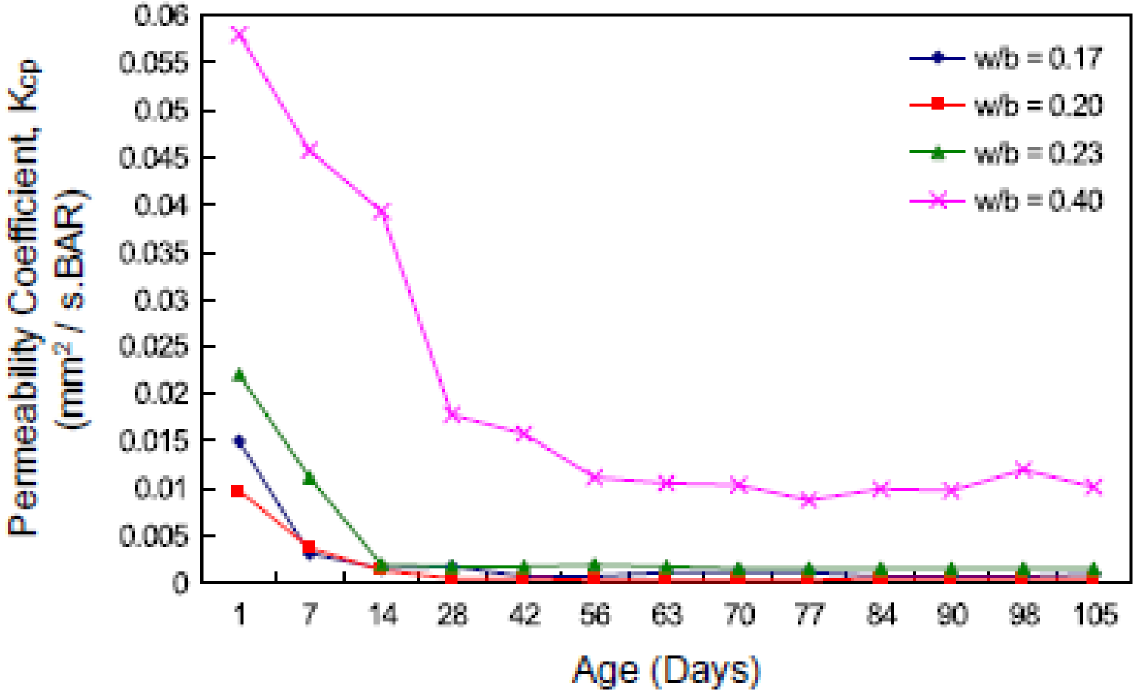

Figure 2.12 Water permeability with different water-to-binder ratios under various ages [51]

For the same investigation it is found that there exists an optimal superplasticizer (SP) dosage which results in the lowest permeability, From Figure 2.13 it is observed that the addition of 2.5% SP gives the lowest permeability coefficient of RPC.

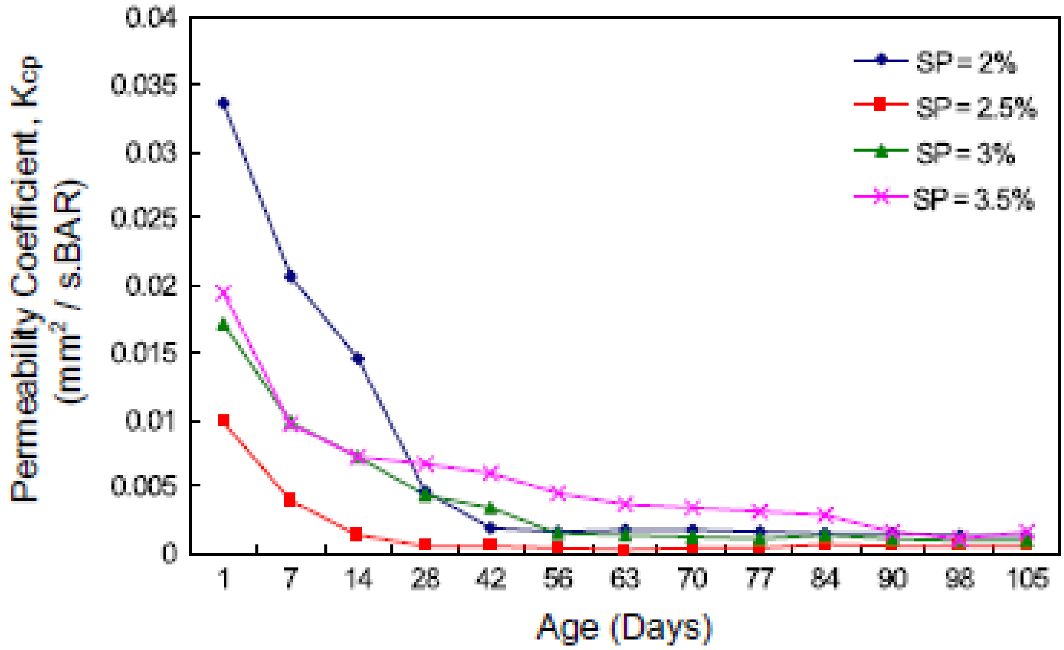

Figure 2.13 Water permeability of RPC with different SP dosages under various ages [51]

From Figure 2.14, it is observed that water permeability of RPC decreases as compressive strength increases across the age. It is also noted from Figure 2.14 that the longer curing time, the higher compressive strength and the lower water penetration are achieved.

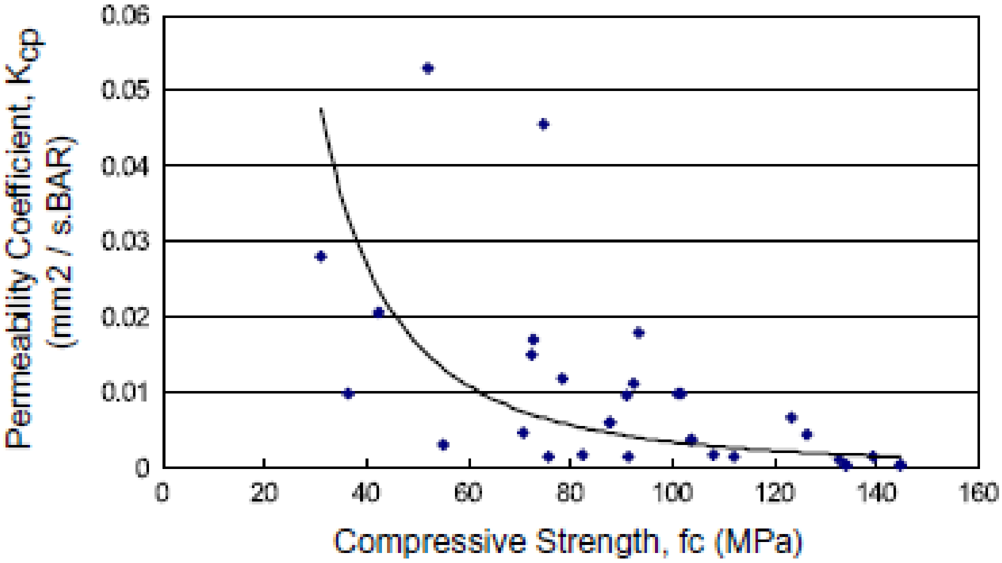

Figure 2.14 Relationships between the permeability and compressive strength for RPC [51]

Wongpa et al. [52] studied the inorganic polymer concretes (IPCs) which were produced from rice husk–bark ash (RHBA) combined with fly ash (FA) as a cementitious raw material. Particle images of both original and ground RHBA are shown in Figure 2.15. The water permeability coefficients for all IPCs increase from 28 days to 90 days, which is opposite from their compressive strength. From Figure 2.16 that the permeability at the same compressive strength of IPCs is much higher than that of conventional concrete; moreover the differences in water permeability become smaller when the compressive strength is higher.

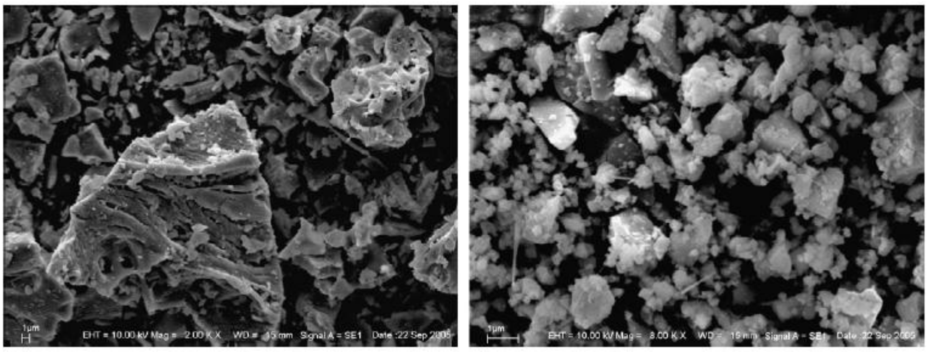

Figure 2.15 Particle images of original and ground RHBA [52]

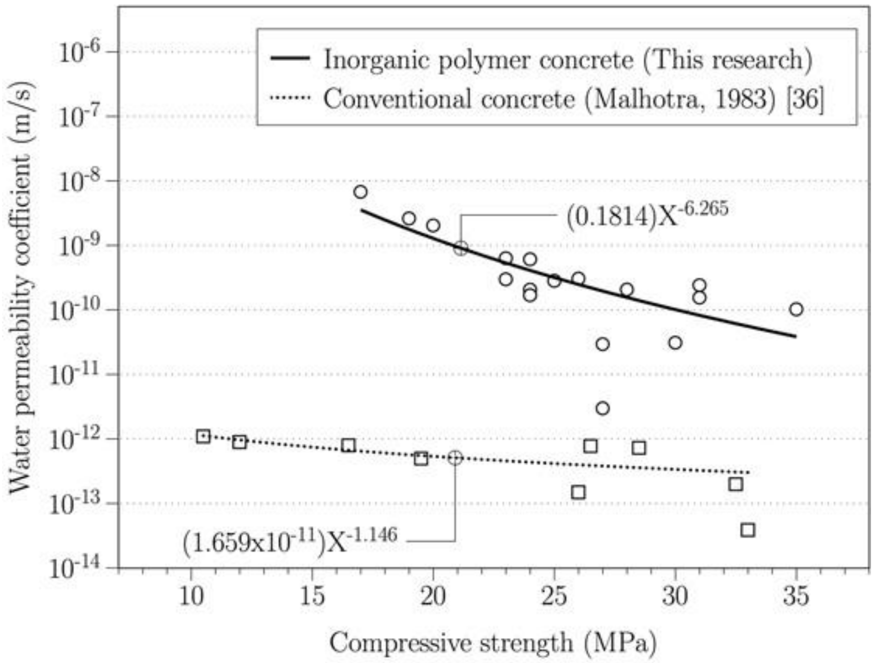

Figure 2.16 Relationship between water permeability coefficient and compressive strength of conventional concrete and IPCs [52]

Park et al. [53] conducted a study on the crack effect on permeation for fully hardened concrete with experimental approaches. The proposed technique is based on the models for early aged concrete. Increasing permeability due to cracking is considered in this technique. From Figure 2.17 that permeability significantly increases for crack widths above 0.2 mm. The increasing permeability ratios in cracked concrete to sound concrete are evaluated to 1.5–2.9 (0.1 mm crack width), 13.6–20.0 (0.2 mm crack width), 37.2–52.2 (0.3 mm crack width), and 747.5–1004.7 (0.4 mm crack width), respectively.

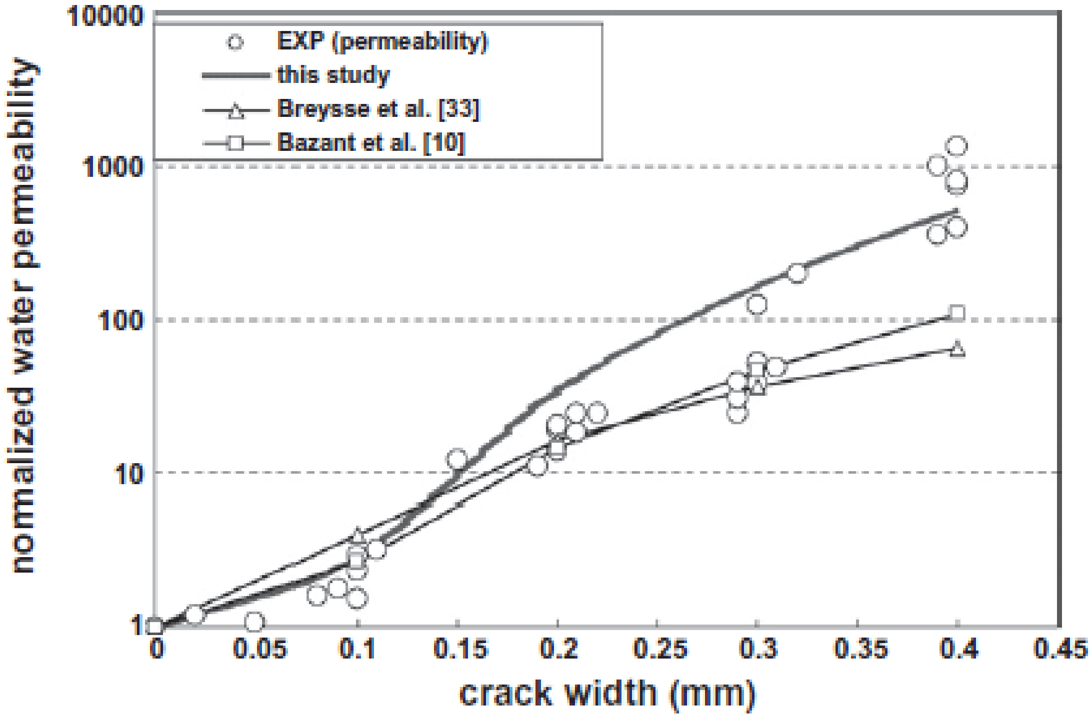

Figure 2.17 Normalized water permeability with crack width including previous models [53]

In the study of Chindaprasirt et al [54], the permeability of ground palm oil fuel ash (GPOA) and ground rice husk–bark ash (GRBA) concretes depends on the cement replacement ratios also the permeability of concrete reduces with the increasing in the compressive strength and age of concrete. The relationship between the permeability of all concretes and the cement replacement levels at 28 and 90 days was drawn. Most of concretes had lower permeability than that of ordinary Portland cement (OPC) for both 28 and 90 days

Also the relationship between compressive strength and water permeability of concrete at 28 and 90 days are presented, the permeability of concrete tended to decrease with the increasing in the compressive strength. It was concluded that, GPOA and GRBA appear to be new cementitious materials to decrease the permeation properties of concrete. On the other hand, the ratio of cement substitution should be taken into account to achieve the concrete with target compressive strength and permeability. Figure 2.18 shows pozzolanic material used in this article.

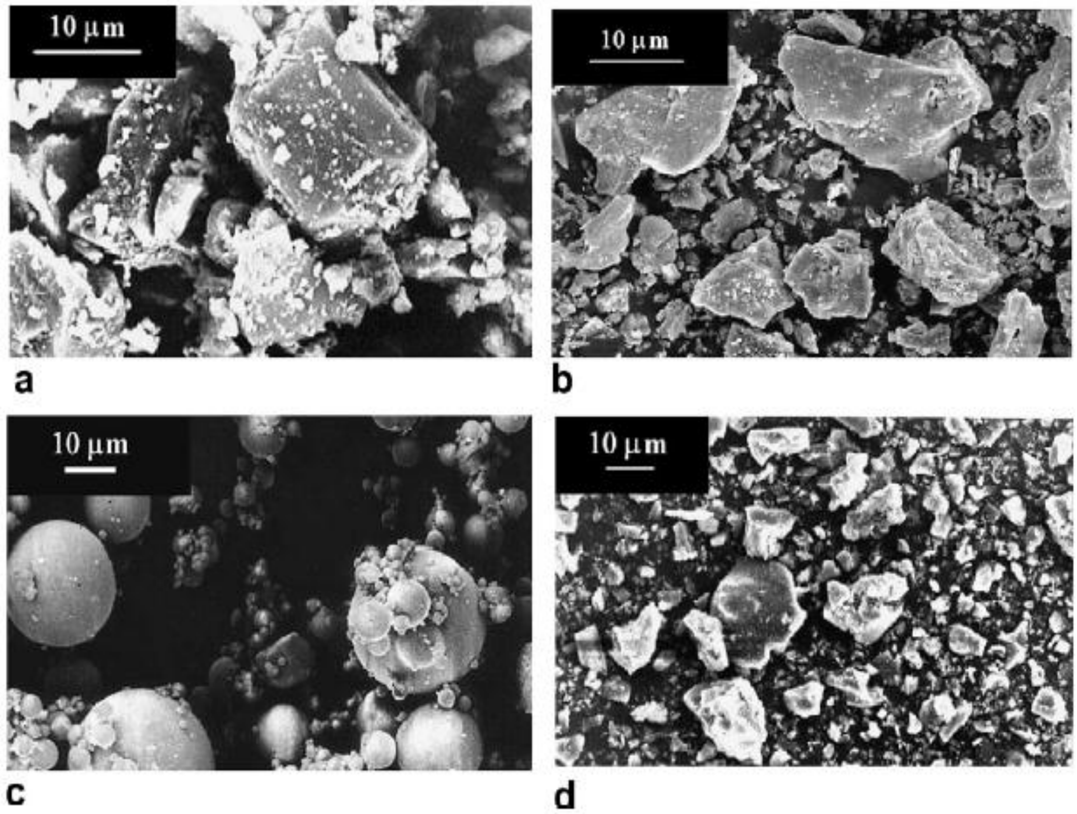

Figure 2.18 Scanning electron microscopy (SEM) of materials: (a) Portland cement type I (OPC); (b) original fly ash (OFA); (c) ground palm oil fuel ash (GPOA); and (d) ground rice husk–bark ash (GRBA).[54]

Tangchirapat et al [55] investigated the use of 10–30% of coarse fineness (CP) and fine fineness (FP) as a cement replacement in ordinary Portland concrete (OPC) and reported a good result in water permeability, depending on the cement replacement level and the concrete age. The water permeability of ground palm oil fuel ash (POFA) concrete decreased as the compressive strength increased. In addition, there was a good correlation between the compressive strength and the water permeability of ground POFA concrete as demonstrated in Figure 2.19.

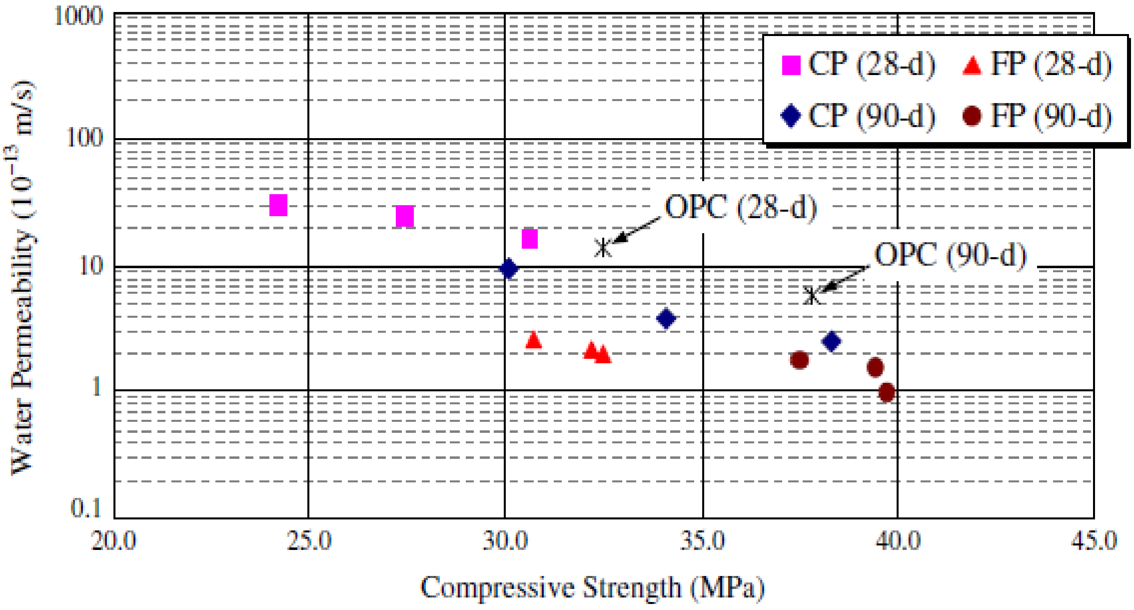

Figure 2.19 Relationship between compressive strength and water permeability of concrete [55]

Yi et al [56] studied the water permeability and how it is affected by hydraulic pressure and crack widths in cracked concrete. When the crack widths were 30 and 50 µm, the water permeability (K_e) value showed a relatively rapid decrease as the hydraulic pressure increased. However, when the pressure increased from 0.01 MPa to 0.025 MPa and the crack width was 100 µm, the K_e value rapidly increased approximately 190 times.

In the study of Mohr et al. [57] an excellent long-term performance in concrete pavements is assessed associated with both concrete strength and durability properties like permeability. Water permeability exhibits a good correlation with compressive strength (R^2=0.73). In Figure 2.20, water permeability at the upper of the concrete is displayed versus compressive strength. It should be notable that there is several different water permeability testing techniques, and that each gives a different range of values and classification levels. This indicates that the measured permeability coefficients test dependent, and do not represent an absolute or intrinsic material characteristic of the concrete.

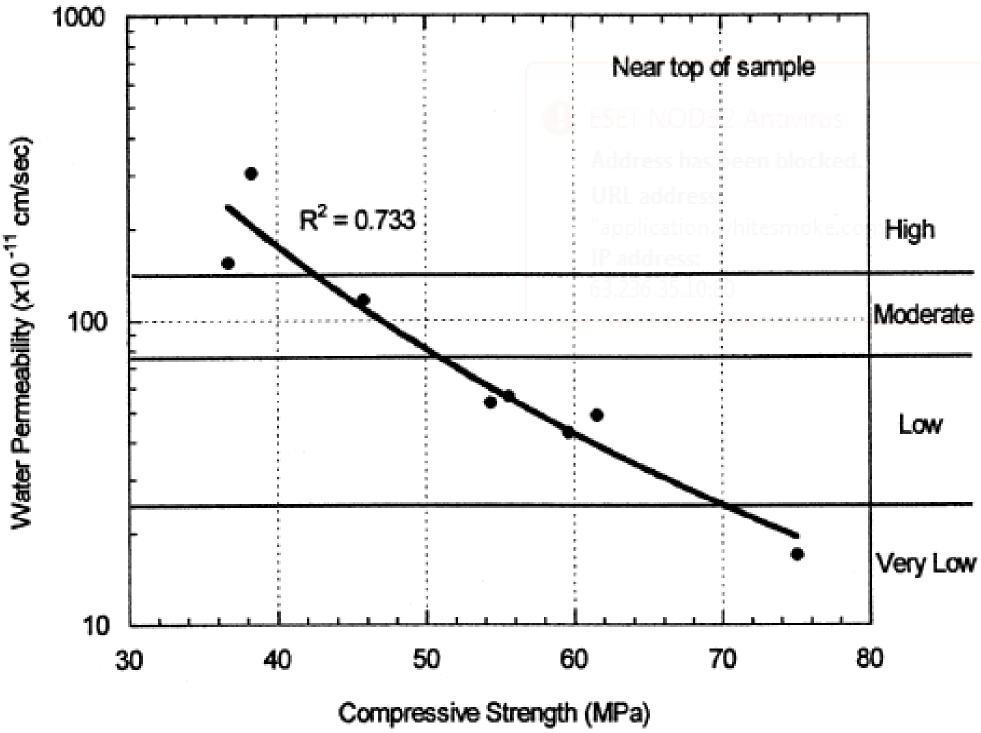

Figure 2.20 Water permeability versus compressive strength for the pavement specimens near the top of the sample, all values are averages for each test section [57]

the transport properties of high-volume fly ash roller compacted concrete (RCC) investigated by Yerramala and Babu [58], The mixes were advanced through incorporating 50–260 kg/m^3 cement and high volumes of fly ash ranging from 40% to 85% by mass of the total cementitious material. The concretes were investigated for water permeability.

The volume of water permeating with time was calculated to assess permeability of the concretes. The mean coefficient of water permeability, obtained from two replicate specimens is shown in Figure 2 21. As shown in Figure 2.21 it can be noticed that low cement, and high fly ash concretes had shown higher permeability

(RCC1 and RCC2). In addition, permeability of high cement and low fly ash concretes (RCC5 and RCC6) was somewhat higher than moderate cement and moderate fly ash concretes (RCC3 and RCC4).

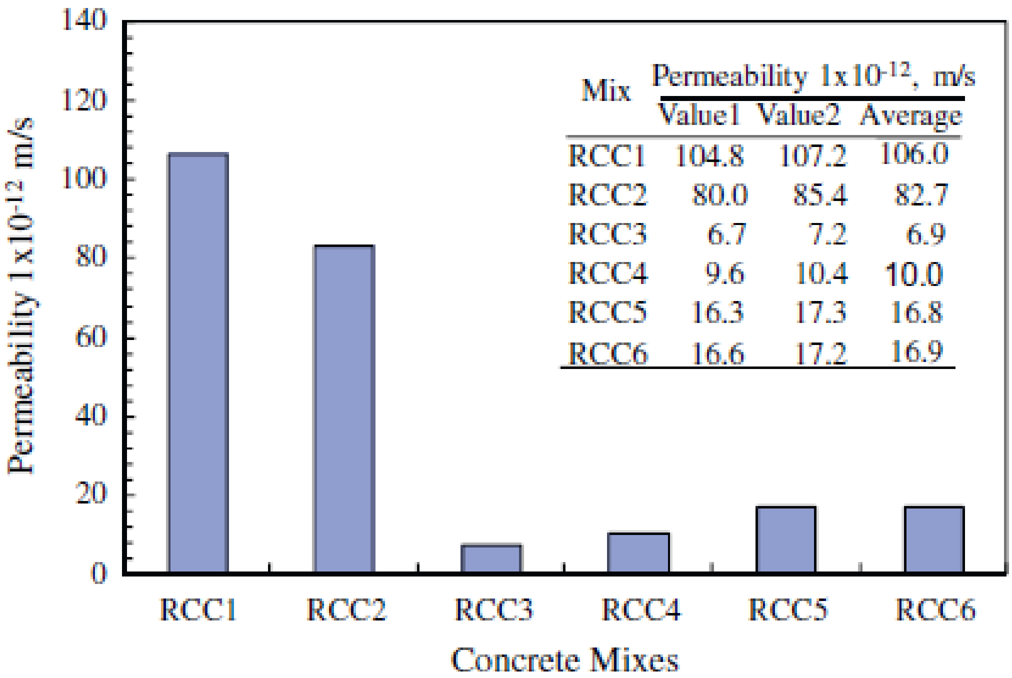

Figure 2.21 Water permeability for the concretes [58]

According to Sonebi and Nanukuttan [59], water permeability test results indicate that the medium strength self-compaction concrete (MSCC) and high-strength self compacting concrete (HSCC) mixtures with pulverized fuel ash (PFA) had the lowest water permeability indexes compared with all other mixtures namely normal, vibrated concretes that may be attributed to their less porous interfacial zone, and also the refined pore structure of the paste matrix of SCC. However, for SCC viscosity modifying admixtures (VMA) demonstrated the highest capillary absorption, which can be attributed to a lack of pore filling effect/capability and higher water-binder ratio (w/b).

The results from investigation of Liu et al. [60] show that the concretes with w/c of 0.38 had comparatively low water permeability regardless of aggregate type and amount of the porous LWA particles used in the concretes. Comparing the concretes with the same w/c, the LWAC indicated higher water permeability than the control concrete. Even though there is generally an improved ITZ between LWA and paste matrix and an improved cement hydration due to internal curing by water absorbed in the LWA leading to reduced capillary pores in LWAC, the LWA is porous and water can enter through the aggregates under pressure. This means that under pressure, the increase in mass of the LWAC can be higher than that of the control concrete. The higher mass increase is related to higher porosity in the LWAC leading to the higher water permeability coefficient.

In the study of Chia and Zhang [61], when comparing between LWC and NWC, they concluded that;

1) Results indicated that at the strength level of about 30–40 MPa the permeability of the LWC was lower than that of the NWC. The lower permeability of the LWC was probably due to a denser interfacial zone between the aggregate and the mortar matrix compared with that of the NWC. In addition the penetration depth for both the high-strength NWC and high-strength LWC was similar.

2) The incorporation of 10% silica fume as cement replacement reduced the water permeability of the concrete, for example; mixes of both LWC and NWC had the water penetration depths that were less than half of those for Mixes of high strength of both LWC and NWC that are without silica fume replacement (respectively).

2.5.2. Rapid Chloride Permeability Test (RCPT)

The conclusion according to Güneyisi et al. [62] revealed that the total charge passed decreased with the utilization of mineral admixtures. The concretes containing binary blends of metakaolin (MK) showed much higher resistance to chloride ion permeability. For example, the total charge passed through the control concrete was nearly 1009 coulombs, which considered the concrete as low. The rank of the concretes changed to be very low. However, for all the concretes with mineral admixtures, the use of MK looked to be the most effective in the lowering of chloride ion permeability, particularly as the effect was raised with increasing MK content. The total charge passed through the concrete made with 15% MK was as low as 164 coulombs; whereas the total charges of the concrete with 60% FA and 60% ground granulated blast-furnace slag (GGBFS) was approximately 715 and 264 coulombs, correspondingly.

About the study of Mohr et al. [57], the average compressive strength for each pavement test part is plotted versus the average of all RCPT data points (Figure 2.22). In each case two to four specimens were tested in strength and RCPT. A power law regression fit of the data yields a good correlation (R^2=0.70). Hence, the regression denotes the compressive strength versus RCPT relation for these concretes regardless of their various mix designs and environmental histories. The importance of this relation comes on various levels. First, it is manifest that the changes in RCPT values are arrested by changes in compressive strength. This is best described by the role the concrete microstructure has on both properties. The manifestation here is that compressive strength can be used as a rough comparative or predictive scale for chloride penetration resistance of ordinary Portland concrete (OPC) pavement concretes. At low and moderate strengths, the decrease in chloride penetration with growing strength is dramatic. By moving from 35 to 45 MPa the ultimate compressive strength, the RCPT results can be expected to reduce from over 4000 to less than 2000 C (a drop of two RCPT classes). While the chloride penetration falls off by moving from 60 to 70 MPa ultimate compressive strength is only a few hundred coulombs within the same RCPT class.

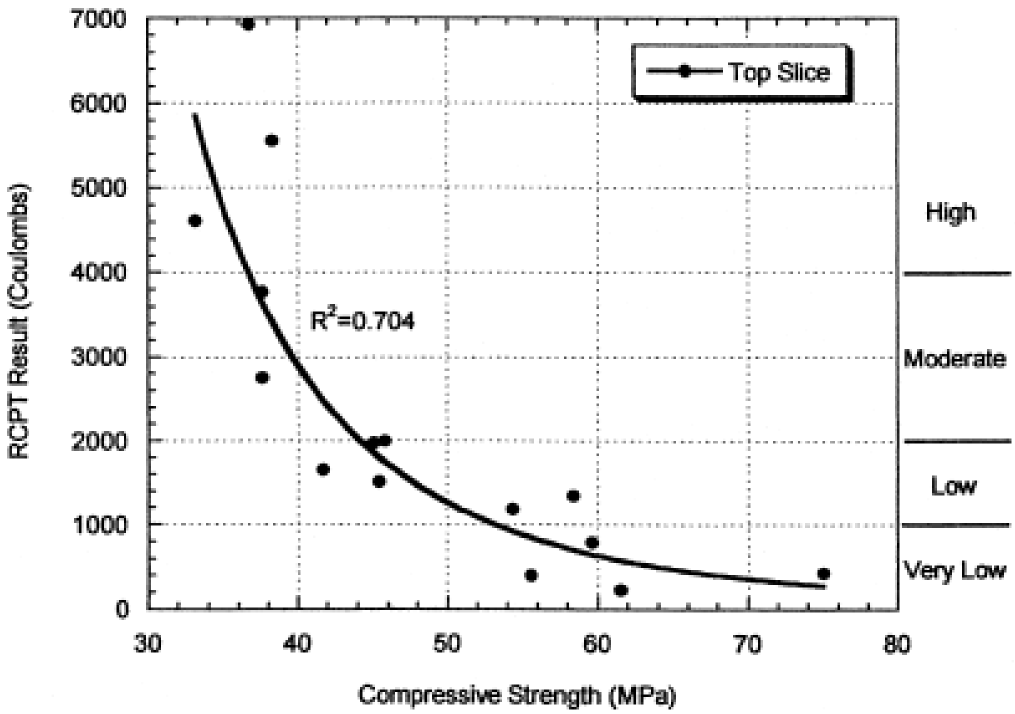

Figure 2.22 Long-term RCPT result versus compressive strength relation for pavement concretes from field study. Permeability values are for the upper portion of the concrete. All values are averages for each test section [57]

From Yerramala and Babu [58] investigation and form Figure 2.23, the chloride ion penetrability limits suggested by ASTM C1202-94 [63]. Assessment criteria were compared with the results. It can be seen that all the concretes showed less than 1000 C total charge passing and these were assessed as (very low). The reduced chloride permeability vales in all the concretes could be attributed to presence of high volumes of fly ash. However, presences of the highest fly ash percentage in RCC1 did not help to reduce chloride permeability than other concretes. The chloride permeability obtained for RCC2 was nearly 48% less than RCC1. Increased cement content and reduced w/(c + f) ratio could have helped to reduce chloride permeability. Contrary, increased cement content in moderate cement and moderate fly ash RCCs (RCC3 and RCC4) and high cement and low fly ash RCCs (RCC5 and RCC6) did not show any appreciable decrease in chloride permeability when compared to RCC2.

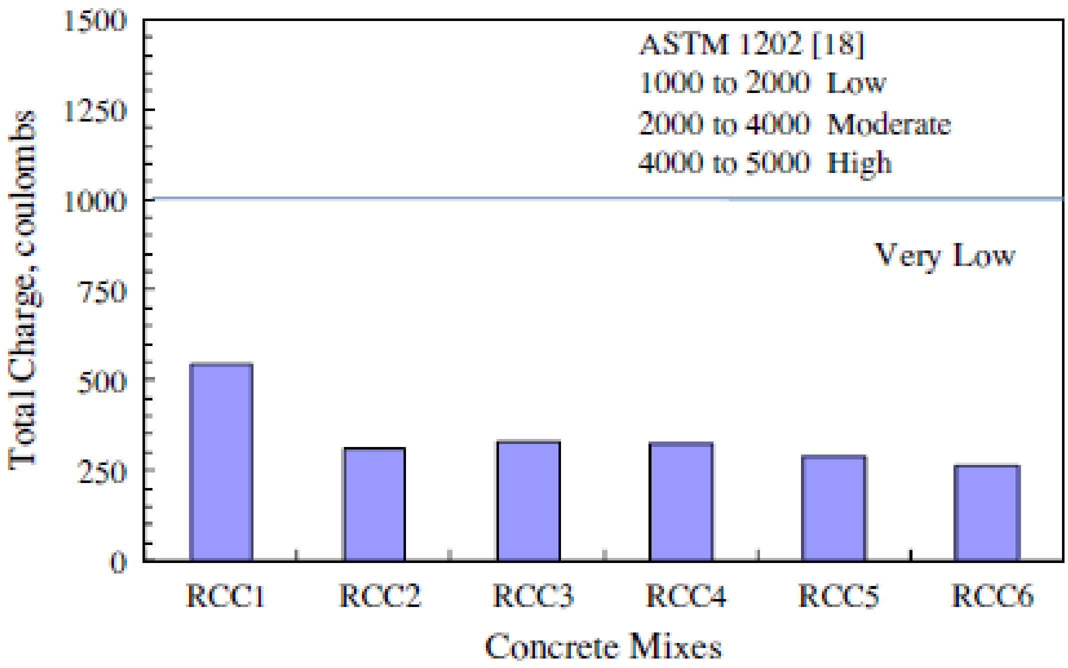

Figure 2.23 Chloride permeability values of the concretes investigated [58]

Liu et al. [60] investigated that LWAC had similar charges passed equated with the control concrete of the same w/c other than for two concrete mixes, which displayed higher charges passed. The charges passed through the concretes, however, were all within the range from 2000 to 4000 coulombs, which was categorized as ‘‘moderate” chloride penetrability according to ASTM C 1202. In the LWAC, LWA had higher porosity compared with the NWA. Nevertheless, the porosity in cement paste in the LWAC was probably lesser due to the internal curing effects compared with that in the NWAC. In addition, the enhancement in the ITZ between LWA and paste matrix in the LWAC also influenced pore structure of the concrete which in turn affected the charges passed.

The study of Chia and Zhang [61] demonstrates an experimental analysis on the chloride penetrability of high-strength lightweight concrete (LWC) in comparison to that of high-strength normal-weight concrete (NWC) with or without the silica fume. The resultant of comparing the chloride-ion penetrability between LWC and NWC with the same proportion by volume (just difference between them was the coarse aggregate used). The resistance of the LWC to the chloride penetration was similar to that of the corresponding NWC both in the normal-strength and high-strength ranks.

As the compressive strength of the LWC was lesser than that of the corresponding NWC, the consequences indicated that for a given 28-day strength, the LWC would obviously have high resistance to water and chloride-ion penetration than the NWC.

2.5.3 Gas Permeability

Care and Derkx [64] described the effect of the microstructure of cementitious materials on the gas permeability. Cement pastes with various water to cement ratios and mortars with two aggregate volume contents have been cast. The microstructure of these materials has been characterized by mercury intrusion porosimetry and gas permeability tests have been carried out with a low-pressure apparatus after preconditioning at controlled relative humidity. Gas permeability relies on upon the mixture (water to cement ratio, aggregate volume content and aggregate size). The gas permeability is correlated to the relative mass loss or the complete porosity for the cement pastes but no correlation can be found for mortars because the aggregate volume content and aggregate size adjust the transport properties in the cement paste matrix.

Picandet et al. [65] investigated experimentally the effect of axial compressive loading on the gas permeability of three various types of concrete: ordinary concrete (OC), high-performance concrete (HPC), and high-performance steel fiber-reinforced concrete (HPFC). Monotonic and cyclic loads are applied on 220×110-mm diameter specimens. Stress levels change between 60% and 90% of the ultimate strength. At the end of the loading stage, a disc is drawn out from the midpoint part of the cylinders and is dried in a ventilated oven. Four different gas permeability tests are conducted during the drying procedure. For every drying stage, the gas permeability of the discs increases with the load-induced strain. Generally, the gas permeability of HPFC is lower than that of corresponding HPCs and it is always lower than the permeability of OC.

The effect of stress on gas permeability in concrete has been explored by Sugiyama et al. [66] using nitrogen gas as the flowing substance. A uniaxial compressive load was assigned to a cylindrical hollow concrete specimen and raised by steps until failure, while the gas flow rate was calculated to calculate gas permeability at each stress level in a steady stage. Gas permeability was later calculated and compared at increasing stress levels. Structural lightweight concrete with water-cement ratios of 0.4 and 0.6 was compared with normal-weight concrete with same water-cement ratios and at similar stress levels. Gas permeability in concrete exposed to oven drying for seven days was constant or lowered slightly up to the time of the stress level reached 45 to 55 % of ultimate strength. In extra of these stress levels, gas permeability started to increase slightly. The effect of compressive stress on gas permeability in concrete came to be significant when the load level reached 76 to 79 % of ultimate strength for normal-weight concrete with the same water-cement ratios, while for structural lightweight concrete, the significant stress level was found to be within the range of 82 to 89 % of ultimate strength. The degree of saturation in concrete was found to have a pronounced effect on gas permeability. Furthermore, degree of saturation affected the gas permeability. A relatively higher degree of saturation resulted in a lesser gas permeability. In addition, as the degree of saturation in concrete became higher, the applied compressive stress was found to have less influence on gas permeability in the concrete even at higher stress levels of about 90 % of the ultimate strength.

The study of Hui-sheng et al. [67] discussed about the Gas permeability of high-performance concrete (HPC) with fly ash (FA) or ground granulated blast furnace slag (GGBFS) and the relationships among them. The relationships between compressive strength and nitrogen gas permeability are shown in Figure 2.24a and b. From the correlation coefficients and correlation trends shown in Figure 2.24, it can be seen that relationships between compressive strength and gas permeability are greatly affected by w/b ratios and sensitive to the blended cementitious systems. For HPC with FA, correlation coefficient values R^2 are 0.88 at w/cm of 0.30 and 0.70 at w/cm of 0.25. For HPC with GGBFS, values of R^2 are 0.73 at w/cm of 0.30 and 0.60 at w/cm of 0.35. It can also be noticed that correlation trends are apparently different for HPC with FA/GGBFS. Compressive strength of HPC with FA is exponentially correlated to the gas permeability coefficient, while it shows a linearly correlated trend for HPC with GGBFS (Figure 2.24)

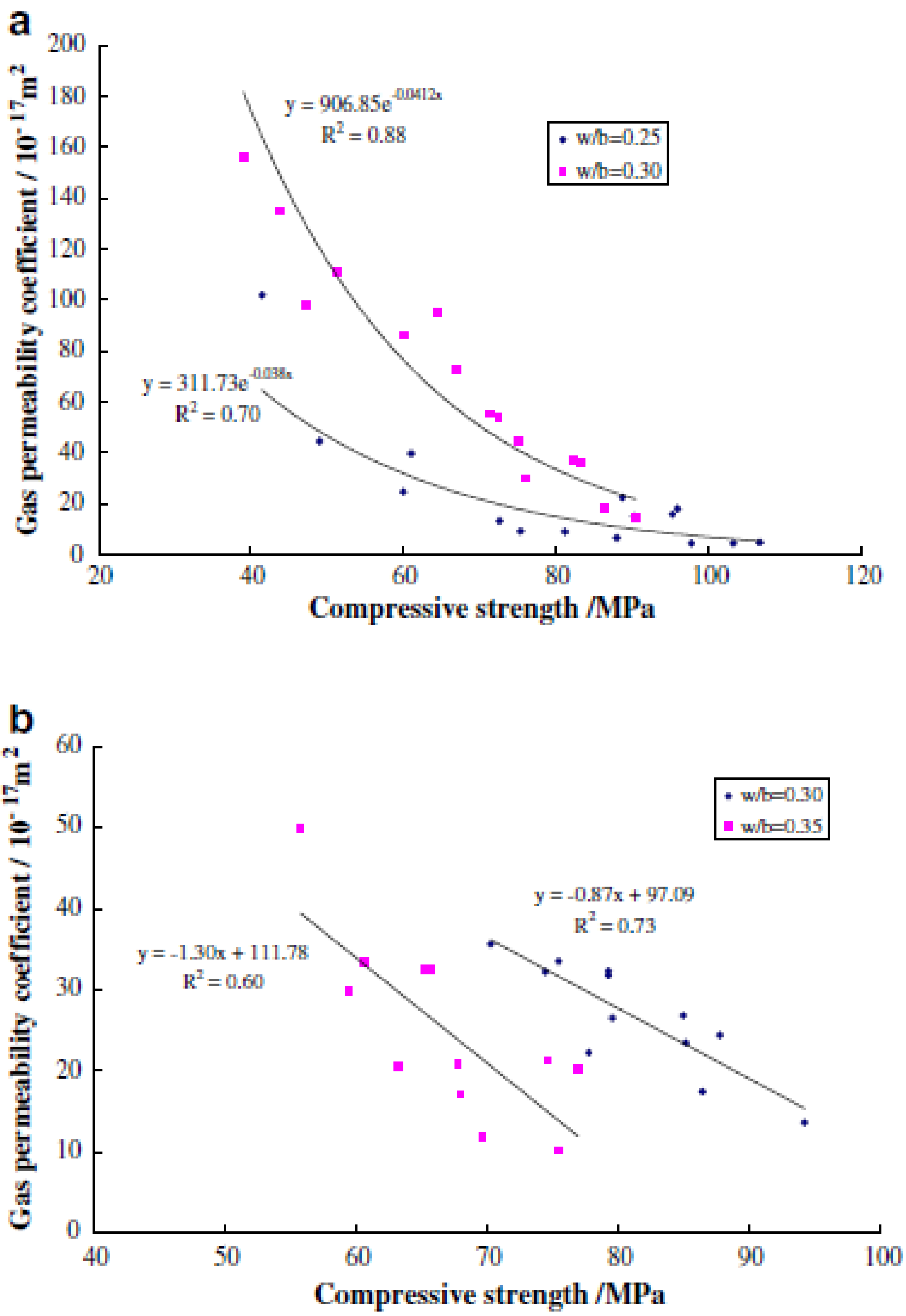

Figure 2.24 Relationship between compressive strength and gas permeability of HPC with FA/GGBFS (a: HPC with FA; b: HPC with GGBFS) [67]

Tsivilis et al. [68] investigated that the clinker quality significantly influences the gas permeability of the limestone cement concrete. It is concluded that, relying on the clinker quality and the cement fineness, limestone cement concrete, with optimum limestone content, can give lower gas permeability as compared with pure cement concrete. Limestone additions can enhance the permeability properties of the concrete, particularly in cements having high C_3A content. The pore size distribution, and more specifically the mean pore size, influences the gas permeability of the concrete. However, in concrete, including cement with clinker of high C_3A value, hydration products precipitate on the aggregate surface, other than it does not affect the permeability properties of the concrete.

Heede et al. [47] concluded that high-volume fly ash (HVFA) mixes with a total binder content of 400 kg/m^3 (50% cement CEM I 52.5 N, 50% fly ash) and a w/b ratio of 0.4 can be significantly less accessible to water and gases (CO2, and O2) than the OPC concrete. The HVFA mix was characterized by 78.9% and 78.0% lesser apparent gas permeability (k_a) at the ages of 28 and 91 days, correspondingly. For both OPC and fly ash concrete, a pronounced linear correlation exists between this gas permeability measured at 2 bar pressure and the total permeable porosity. Plotting the square root of k_a as a function of the concrete's dryness, gives a pronounced linear correlation and makes it practicable to calculate the gas permeability corresponding with the saturation degree of the concrete in equilibrium through the environment.

2.5.4 Sorptivity Test

In the investigation of Guneyisi and Mermerdas [69], the variation in sorptivity with w/b ratio, concrete age, and curing condition for the plain and MK-modified concretes are given in Figure 2.25. It is obvious that sorptivity reduces systematically with an increase in curing time, and the gradient of the sorptivity tends to reduce with an increase in the replacement level of MK. At 28 days, the sorptivity values are obviously reflected in the strength values. Increasing the MK content reduced both the 28 and 90-day sorptivities of the concrete for the 0.55 w/b ratio and water-cured concretes. The sorptivity values of the concrete including MK were approximately from 2% to 36% and from 8% to 60% lower than that of the plain concretes at 28 and 90 days, correspondingly, depending on w/b ratio, the amount of MK used, and curing regime.

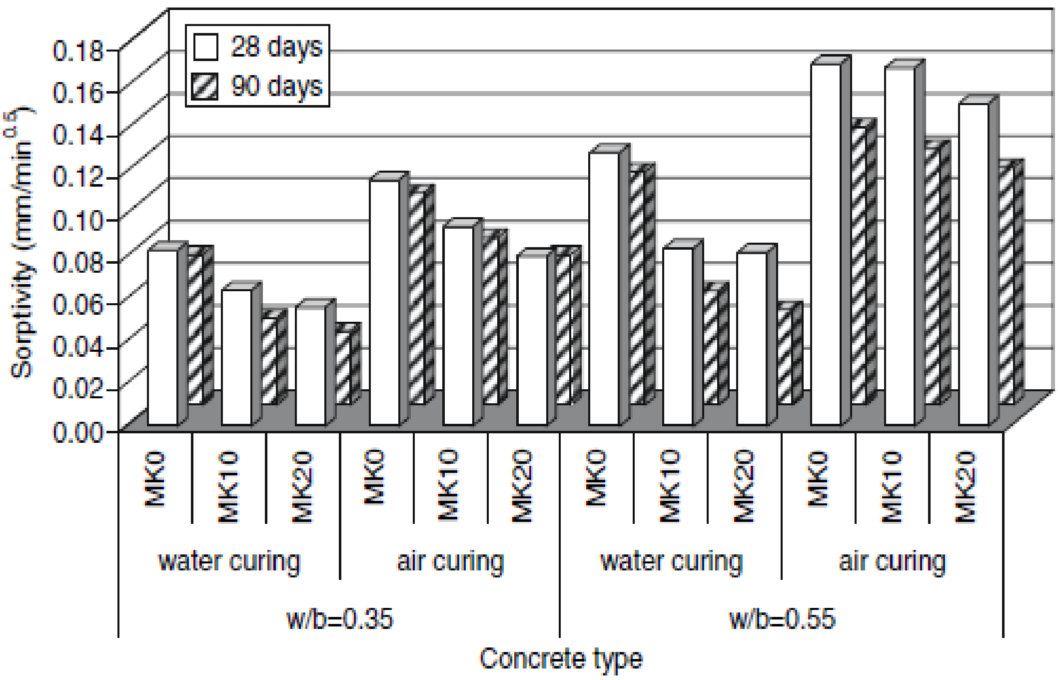

Figure 2.25 Variation in sorptivity of plain and MK-modified concretes to different curing regimes [69]

According to Güneyisi et al. [62], Figure 2.26 displays the normalized water sorptivity of the concretes with respect to the control specimen. The sorptivity test consequences of the produced SCCs measured at 90 days. The plain control concrete had the highest sorptivity. Incorporating the mineral admixtures, continuously decreased the sorptivity of the SCCs, the lowest sorptivity index was measured for the concretes with the ternary blends of 15% MK and 45% GGBFS and the binary blends of 15% MK. The use of MK seemed to be much more effective in reducing the sorptivity due to the reduced pore volume. Using FA and/or GGBFS with MK gave a marked decrease in the sorptivity as well.

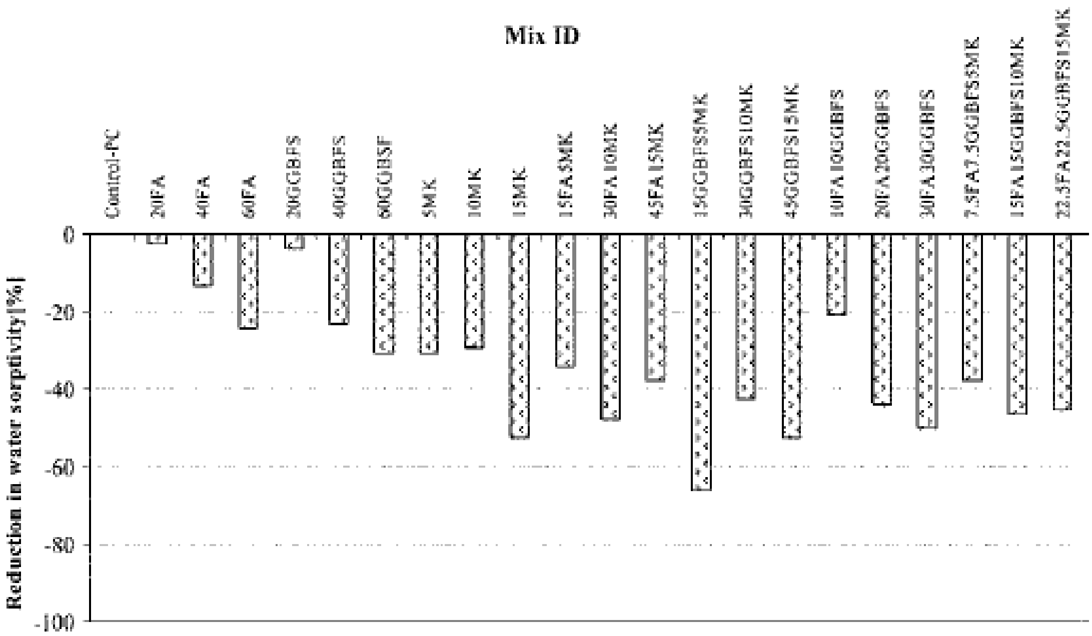

Figure 2.26 Normalized water sorptivity of concretes with respect to control specimen [62]

According to study Bai et al. [70] the variation in sorptivity with age of the water-cured metakaolin–pulverised fuel ash (MK–PFA) and Portland cement–pulverised fuel ash–metakaolin (PC–PFA–MK) concrete for all cement replacement levels (10%, 20%, 30% and 40%) cured up to 18 months are given in Figure 2.27. In each situation, sorptivities are compared with those of the control PC concrete. Clearly sorptivity reduces systematically with an increase in curing period, and the gradients of the sorptivity versus age curves tend to reduce with an increase in MK content (Figure 2.27a and c). Moreover, at 28 days, the relevant sorptivity values are clearly reflected in the strength prices. Thus, the water-cured concretes with the highest sorptivities have the lowest strengths (i.e. the PC–PFA blended), as well as the concretes with the lowest sorptivities have the highest strengths (i.e. the PC–PFA–MK blends with the highest MK content).

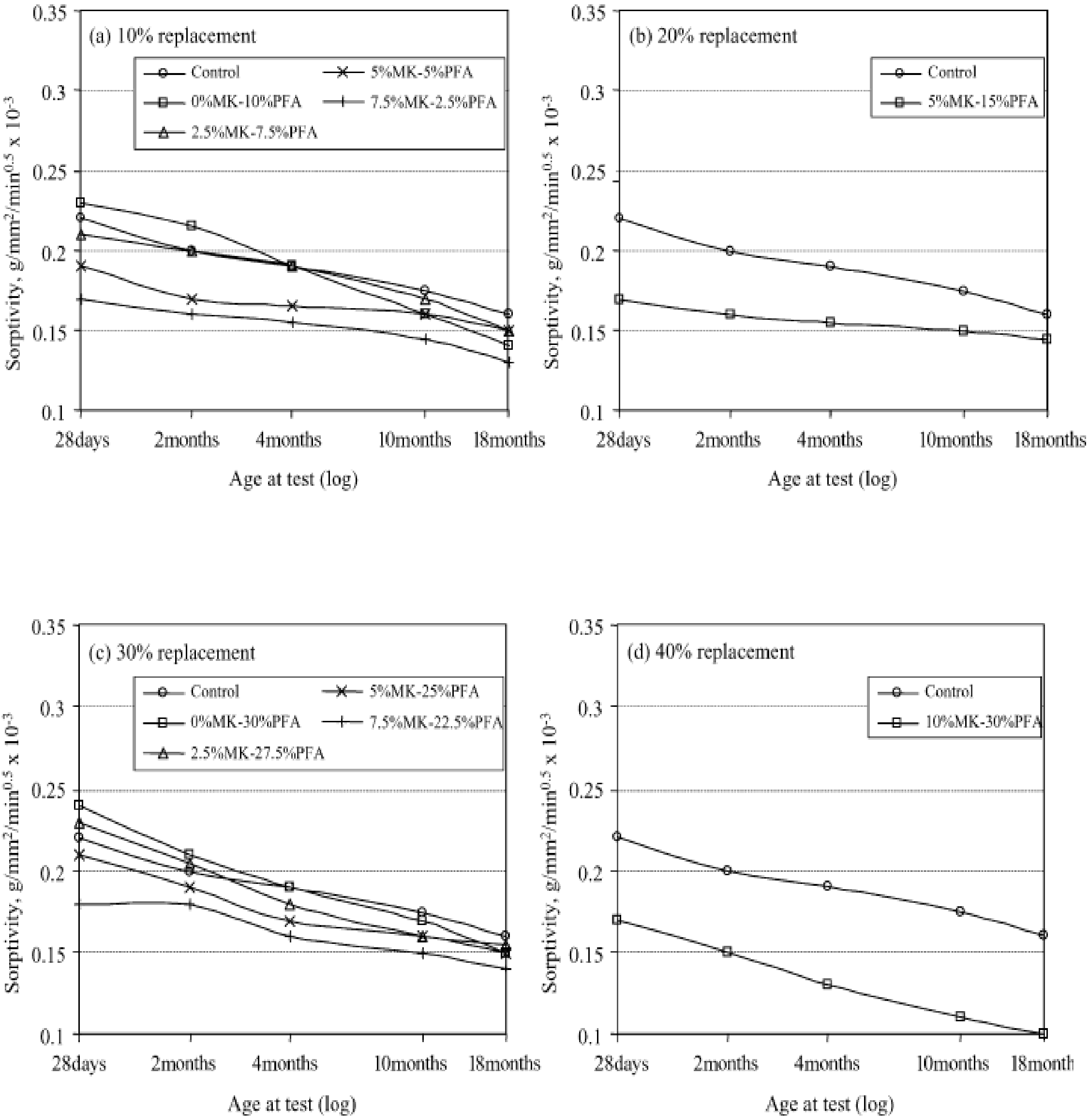

Figure 2.27 Sorptivity with age at 10%, 20%, 30% and 40% cement replacements for water-cured concrete [70]

Yerramala and Babu [58] concluded the sorptivity of the low cement and high fly ash RCCs (RCC1 and RCC2) was higher than another concrete. Furthermore, it can also be seen that sorptivity of high cement and low fly ash RCCs (RCC5 and RCC6) was closely same as that of moderate cement and moderate fly ash RCCs (RCC3 and RCC4). As for permeability increase in cement content did not display any significant decrease in sorptivity in RCC5 and RCC6. Figure 2.28 gives a comparison between sorptivity and permeability of the concretes, nevertheless, of the amount of cement, fly ash percentage, total cementitious material and w/(c + f). In general, very good correlation is noticed between the sorptivity and the permeability values. As both the parameters are functions of the porosity and pore system, permeability increased with sorptivity. Sorptivity of the concretes is demonstrated in Figure 2.29.

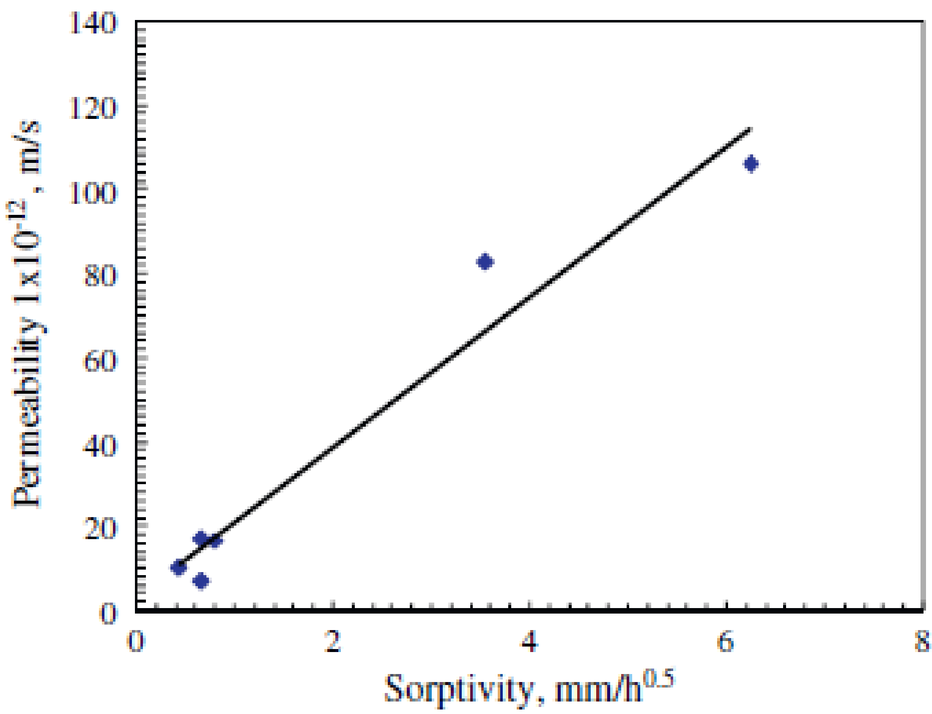

Figure 2.28 Relationship between permeability and sorptivity [58]

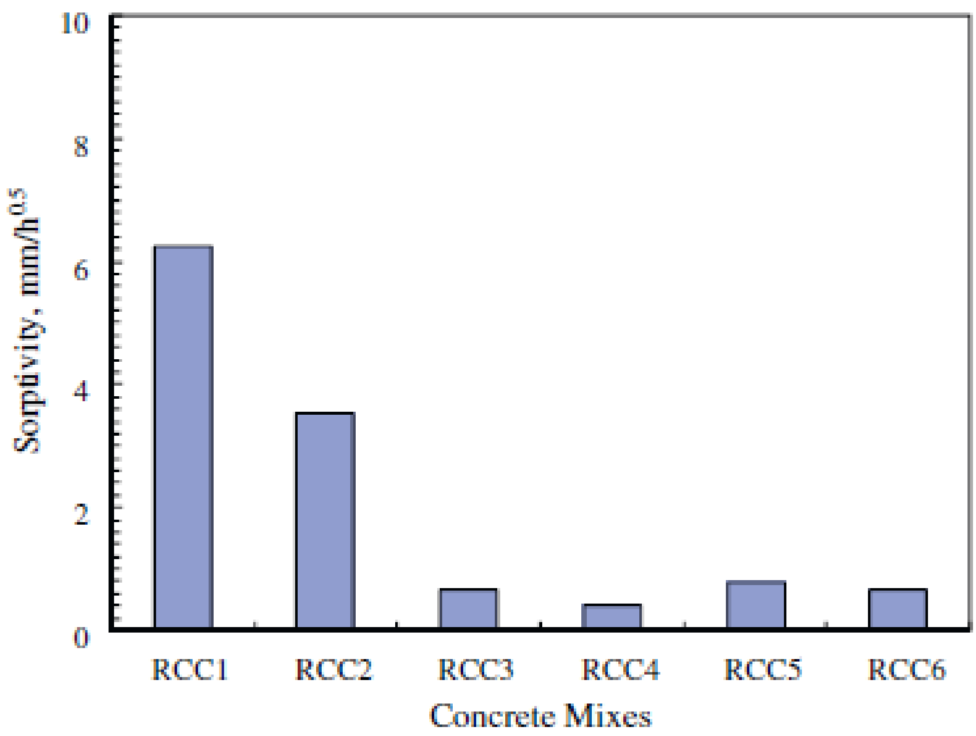

Figure 2.29 Sorption characteristics of the concretes [58]

CHAPTER 3

EXPERIMENTAL STUDY

3.1. Materials

3.1.1. Cement

Ordinary Portland cement was used in this study (Portland cement CEM, I 42.5R) conforming to the TS EN 197-1 [71] (which mainly based on the European EN 197-1). It had a specific gravity of 3.15 g/cm^3 and Blaine fineness of 326 m^2/ kg. It was utilized in the production of both artificial aggregates and concretes. Physical and chemical properties of the cement and fly ash are given in Table 3.1.

Table 3.1 Chemical compositions and physical properties of Portland cement and fly ash

Analysis Report (%)	Cement	Fly ash
CaO	62.58	4.24
SiO_2	20.25	56.2
Al_2O_3	5.31	20.17
Fe_2O_3	4.04	6.69
MgO	2.82	1.92
SO_3	2.73	0.49
K_2O	0.92	1.89
Na_2O	0.22	0.58
Loss on ignition	3.02	1.78
Specific gravity (kg/lt)	3.15	2.25
Blaine fineness(m^2/kg)	326	287

3.1.2. Fly Ash

Fly ash (FA) used in the manufacture of lightweight aggregates was a class F type according to ASTM C 618 (2002) [22] was supplied from Ceyhan Sugözü thermal

Power Plant. It had a specific gravity of 2.25 g/cm^3 and the Blaine fineness of 287 m^2/ kg. Physical and chemical properties of the fly ash is given in Table 3.1.

3.1.3. Superplasticizer

A superplasticizer (SP) with a specific gravity of 1.22 g /cm^3 was used to achieve the target workability. The properties of superplasticizer are given in Table 3.2

Table 3.2 Properties of Super Plasticizer

Property	Superplasticizer
Name	Daracem 200
Colour	Dark Brown
State	Liguid
Specific Gravity [kg/lt]	1.22
Chemical	Sulfonated Naphthaline Formaldehyde
Freezing Point	-4

3.1.4. Aggregates

3.1.4.1. Lightweight Aggregates (LWAs)

Artificial lightweight fly ash aggregates (LWAs) produced through a cold bonding process was used in manufacturing of LWCs. For this, dry fine particle's mixture of fly ash and Portland cement in particularized proportions was pelletized through moisturizing in a rotating inclined pan at an ambient temperature. The pelletizer used has a pan diameter of 80 cm and a depth of 35 cm (Figure 3.1). A typical manufacture period seized about 20 min while the water was sprayed throughout the initial 10 min on the fly ash–cement fine particles mixture to act as a binder. Quantity of sprayed water was about 18-20 % by weight of the dry powder mixture. The second half of the pelletization period was devoted to the further stiffening of the fresh pellets (Figure 3.2). Subsequently, they were maintained in sealed plastic bags and stored for hardening in a curing room at a temperature of 20 ^{o}C and a relative humidity of 70% for 28 days [14] as shown in Figure 3.3, thereafter the hardened fly ash aggregates was sieved into fractions of 4-14 mm sizes to be used in LWC production (Figure 3.4). In determining properties of LWA, specific gravity and the water absorption tests were carried out as per ASTM C127 [72], while crushing strength test was performed as per BS 812, part 110 [73]. It was found that water absorption after 24 hr. was 12.7% while specific gravity of LWA for bulk; apparent and saturated surface dry conditions were 1.73, 2.32, and 1.98 g /cm^3 respectively. Moreover, crushing strength of LWA is shown in Figure 3.5.

Figure 3.1 The general view of the pelletization disc

Figure 3.2 Fresh artificial lightweight aggregates

Figure 3.3 The aggregates kept in sealed plastic bags

Figure 4.5 Sieved artificial lightweight aggregates

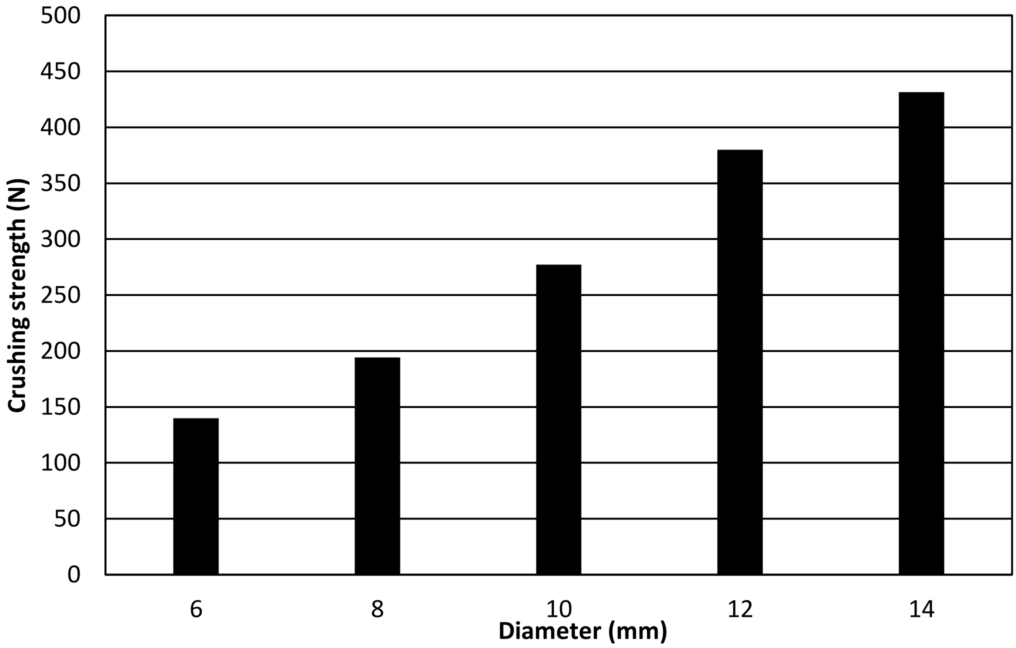

Figure 3.5 Crushing strength of LWA

3.1.4.2. Normal Weight Aggregates

A mixture of natural fine and coarse aggregate was used to produce the NWCs. Sieve analysis and physical properties of both aggregates are shown in Table 3.3. Moreover, LWCs included natural fine aggregates apart from the artificial lightweight coarse aggregates.

Table 3.3 Sieve analysis and physical properties of normal weight aggregate

Sieve size (mm)	**Fine aggregate (%)**		**Natural Coarse aggregate (%)**	
	River sand	Crushed sand	No I	No II
31.5	100	100	100	100
16.0	100	100	100	27.7
8.0	99.7	100	31.5	0.6
4.0	94.5	99.2	0.4	0
2.0	58.7	62.9	0	0
1.0	38.2	43.7	0	0
0.50	24.9	33.9	0	0
0.25	5.40	22.6	0	0
Fineness modulus	2.79	2.38	5.68	6.72
Specific gravity (gr/cm^3)	2.66	2.45	2.72	2.73

3.2. Concrete Mixture Details

To investigate transport properties of NWC and LWC, four mixes were developed according to designed compressive strength of 25 and 45 MPa. Out of the four mixes, two were created for the normal weight concrete, namely, NWC25 and NWC45 and the others were designed for the lightweight concretes, namely LWC25 and LWC45. Water per cement ratio was 0.35 and 0.60 for the designed compressive strength of 25 and 45 MPa, respectively. The slump test was carried out in accordance with BS EN 12350-2 [74] and the test results were in the range of 15±2 mm. Details for concrete mixes are presented in Table 3.4. It can be noted from Table 3.4 that the superplasticizer was used at varying amounts to provide the desired workability.

Table 3.4 Concrete mix design

Code Number	w/c	Cement kg/m^3	Water kg/m^3	SP kg/m^3	Coarse Aggregate kg/m^3			Fine Aggregate kg/m^3		Density kg/m^3
					No 51	No 51	LWA	Crush sand	Natural sand	
LWC25	0.55	350	192.5	1.4			668.14	248.0	625.96	2086.0
NWC25	0.6	300	180	1.2	384.1	667.25		86.18	748.50	2367.2
LWC45	0.35	450	157.5	8.55			665.46	247.0	623.45	2152.0
NWC45	0.45	370	166.5	4.07	378.0	656.67		84.81	733.87	2393.9

3.3. Specimen Preparation and Curing

All concretes were mixed in accordance with ASTM C192 [75] standard in a power driven rotating pan mixer with a 20 L capacity. All samples were poured into the steel moulds in two layers, each of which being vibrated for a couple of seconds. After casting the moulded specimens were protected with a plastic sheet and left in the casting room for 24 hr. Thereafter, the samples were demolded and cured in water until the testing ages.

3.4. Test Methods

3.4.1. Compressive Strength

The compression test was carried out on the specimens by a 3000 kN capacity testing machine. Compressive strength test was conducted at the ages of 7, 28 and 56 days on three 150 mm cube samples for each concrete mixture with respect to ASTM C 39 [76].

3.4.2. Water Permeability

TS EN 12390-8 [77] was followed in the determination of the water permeability of the concretes. For this, a 500 ± 50 kPa downward pressure was applied on the 150 mm cube specimen for 72 hours to penetrate drinkable water throughout the specimen as seen in Figure 3.6. At the end of the 72 hrs period, the test specimens were split in the middle and the greatest penetration depth of pressurized water was measured in mm. Test was conducted at the age of 28 and 56 days and the average of two test specimens is presented in the study.

Figure 3.6 Water permeability test set up

3.4.3. Chloride Ion Permeability

The rapid chloride permeability test (RCPT) was conducted in order to determine the resistance of the concrete to the penetration of chloride ions according to AASHTO T277 [78]. Two specimens of Ø100x200 mm dimensions were tested simultaneously for each concrete at the end of 28 and 56 day curing periods. After curing, two 50 mm thick disc samples were cut from the middle of each cylinder and were conditioned as mentioned in AASHTO T277. Then, the disc specimens were transferred to the test cell in which one face of the specimen was in touch with 0.30 N NaOH solutions and the other was with 3% NaCl solution. A direct voltage of 60.0 ± 0.1 V was applied across the faces (Figure 3.7 and 3.8). A data logger registered the current passing through concrete over a 6 hour period. Terminating the test after 6 hours, current (in amperes) versus time (in seconds) were plotted for each concrete and the area underneath the curve was integrated to obtain the charge passed (in coulombs). AASHTO T277 classifies the chloride permeability in concrete into five classes from 'High' to 'Negligible' on the basis of the coulomb, as tabulated in Table 3.5.

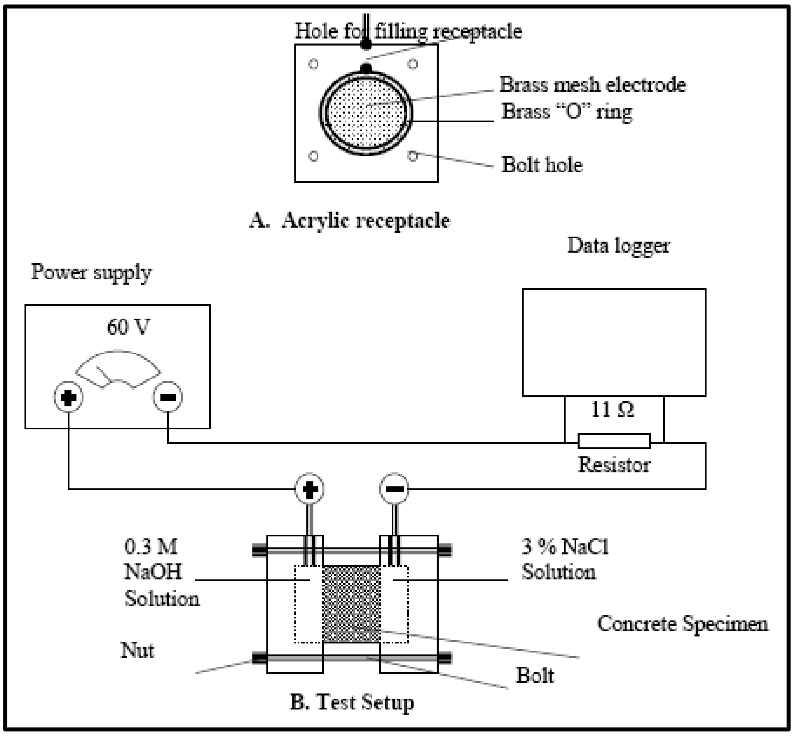

Figure 3.7 Schematic presentation of the test set up for RCPT

Figure 3.8 Rapid chloride permeability tests

Table 3.5 Interpretation of results obtained using RCPT test

Charge Passed (Coulombs)	Chloride Permeability	Typical
>4000	High	High w/c ratio (< 0.6) conventional Portland cement concrete
2000 – 4000	Moderate	Moderate w/c ratio (0.4 – 0.5) conventional Portland cement concrete
1000 – 2000	Low	Low w/c ratio (< 0.4) conventional Portland cement concrete
100 – 1000	Very Low	Latex-modified concrete, Internally sealed concrete
< 100	Negligible	Polymer-impregnated concrete, Polymer concrete

3.4.4. Gas Permeability

The CEMBUREAU method recommended by RILEM TC 116 [79] was used for investigating the gas permeability of the different concrete mixtures. The photographic view and the schematic layout of the apparatus as well as the detail of the testing cell are shown in Figure 3.9, Figure 3.10 and Figure 3.11. The gas permeability of the concrete samples was measured on 50 mm height and 150 mm diameter concrete disk specimens cut from the mid portion of Ø 150x300 mm cylinder. Oxygen gas was used as the permeating medium. Differential pressures varying from 150 to 500 kPa were applied to the specimens in pressure cells which were sealed by a tightly fitting rubber pressuring under high pressure against the curved surface. Prior to the gas permeability test, oven drying process was processed. For gas permeability test, when curing period of 28 day was ended, the specimens would be dried at 105 ^{o}C in oven to make sure each specimen weight change was less than 1%. Then, they were kept in a sealed box till test began. Two specimens for each concrete mixture were tested at the age of 28 days and the average of them was reported as a test result.

For each differential pressure from 150 to 500 kPa, Hagen-Poiseuille relationship [65] for laminar flow of a compressible fluid through a porous media with small capillaries under steady-state condition was used to determine the apparent gas permeability coefficient K_A [65], which can be calculated using the modified Darcy's equation:

$$K_A = \frac{2P_2QL\mu}{A(P_1^2 - P_2^2)} \tag{1}$$

Where K_A is the gas permeability coefficient (m^2), P_1 is the inlet gas pressure (N/m^2), P_2 is the outlet gas pressure (N/m^2) A is the cross-sectional area of the sample (m^2), L is the height of sample (m), μ is the viscosity of oxygen 2.02×10^{-5} Ns/m^2, and Q is the volume flow rate (m^3/s).

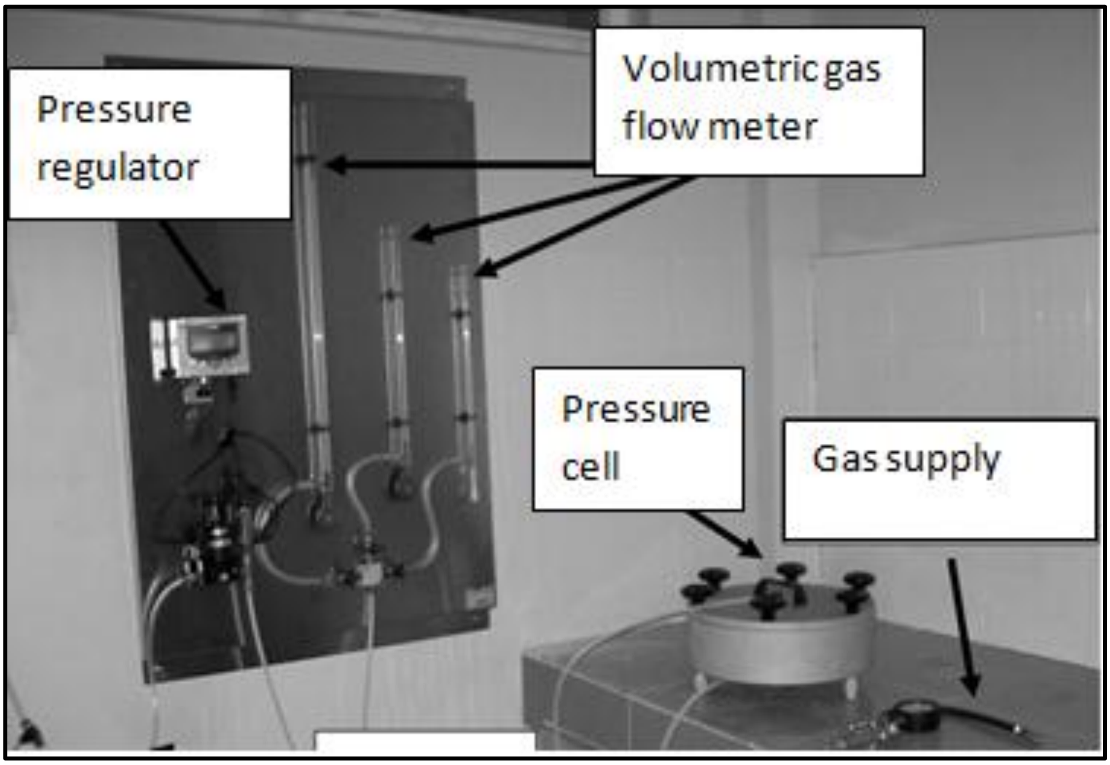

Figure 3.9 Photographic view of the gas permeability test set up and details

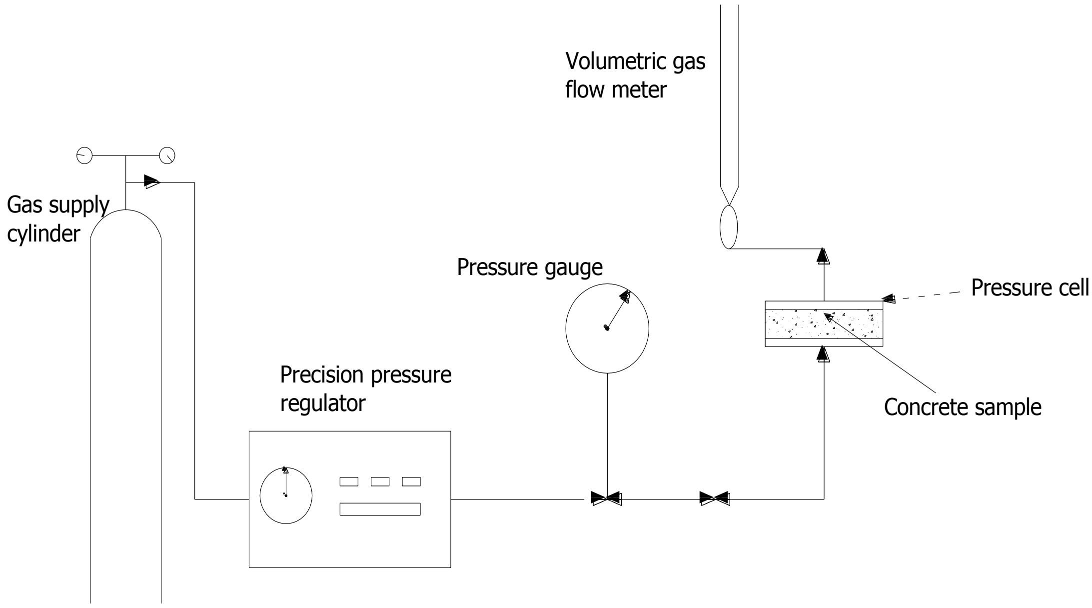

Figure 3.10 Schematic presentation of the gas permeability test set up

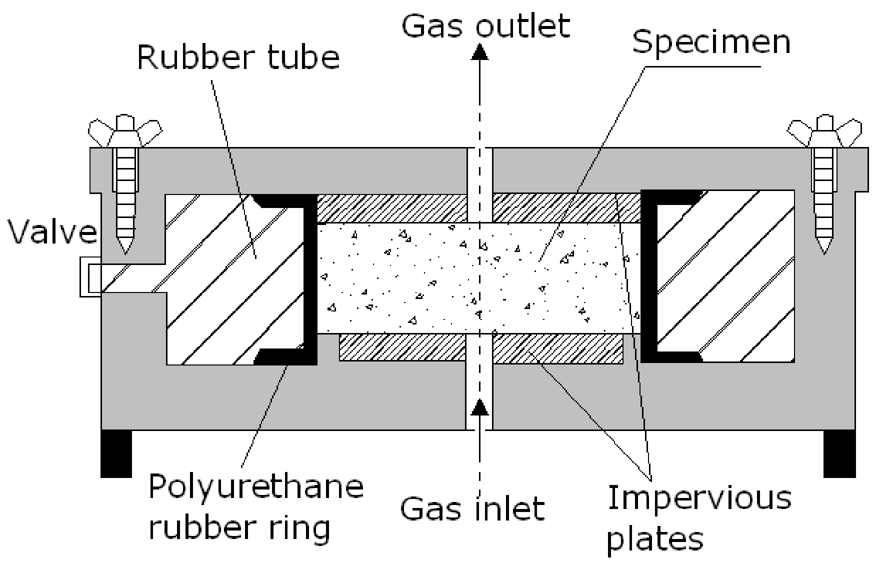

Figure 3.11 Schematic presentation of the pressure cell and test specimen

3.4.5. Sorptivity Index

A sorptivity test measures the rate at which water is drawn into the pores of concrete as per ASTM C 1585.[80] for this test, three specimens with dimensions of Ø100x75 mm cut from Ø100x200 cylinders were employed. At the age of 28 and 56 days, specimens were first dried in an oven at about 50 ^{o}C until constant mass and then allowed to cool to ambient temperature in a sealed container. Afterwards, the sides of the specimens were coated by paraffin and the sorptivity test was carried out by placing the specimens on glass rods in a tray containing water such that their bottom surfaces were 5 mm deep in water, thus allowing free movement of water through the bottom surface [69] as demonstrated in Figure 3.12. The specimens were removed from the tray and weighed at different time intervals up to 24 hours to evaluate the mass gain. The volume of water absorbed was calculated by dividing the mass gained by the nominal surface area of the specimen and by the density of water. These values were plotted against the square root of time. The slope of the best fit line was defined as the sorptivity coefficient of concrete [81].For each properties of the concrete, three specimens were tested and the average of them was reported as the sorptivity coefficient.

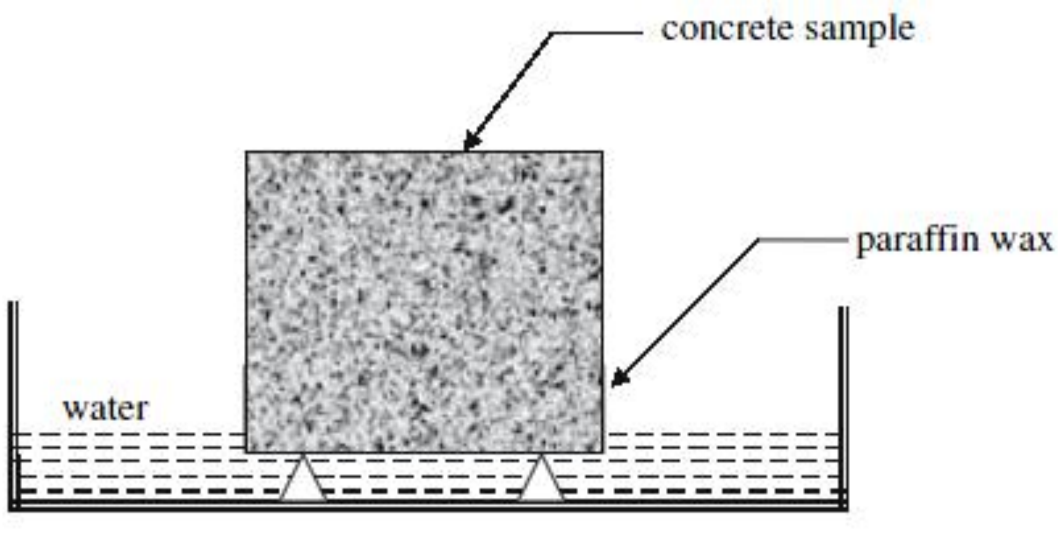

Figure 3.12 Measurement of concrete sorptivity

CHAPTER 4

TEST RESULTS AND DISCUSSIONS

4.1. Compressive Strength

Variations in the compressive strength of normal and lightweight concretes measured at 7, 28 and 56 days are tabulated (Table 4.1) and presented in Figure 4.1. It was observed that the early compressive strength of LWC at 7 days of curing was about 6 % lower than that of NWC while the reduction of the former with respect to the latter was 8% at 28 days. At 56 days, however, LWC25 and LWC45 had lower compressive strengths than NWC25 and NWC45 by about 14% and 5%, respectively. Lowering the w/c ratio enhanced the compressive strength for both LWCs and NWCs. However, this beneficial effect was less for LWCs inasmuch as the further improvement of the matrix did not necessarily mean higher compressive strength for concrete due to the earlier failure of the lightweight coarse aggregate particles. In the study of Chia and Zhang [61], a similar finding was reported such that the LWCs had remarkably lower strength values than those of NWCs for both w/c ratios of 0.35 and 0.55. Indeed, the strength increase was as high as 35% for the low w/c ratio.

Table 4.1 Compressive strength values of NWC and LWC

Code Name	**Compressive Strength (MPa)**		
	7 DAYS	**28 DAYS**	**56 DAYS**
LWC25	22.9	26.5	30.0
NWC25	24.1	28.8	35.1
LWC45	38.8	43.6	47.5
NWC45	41.2	47.4	50.0

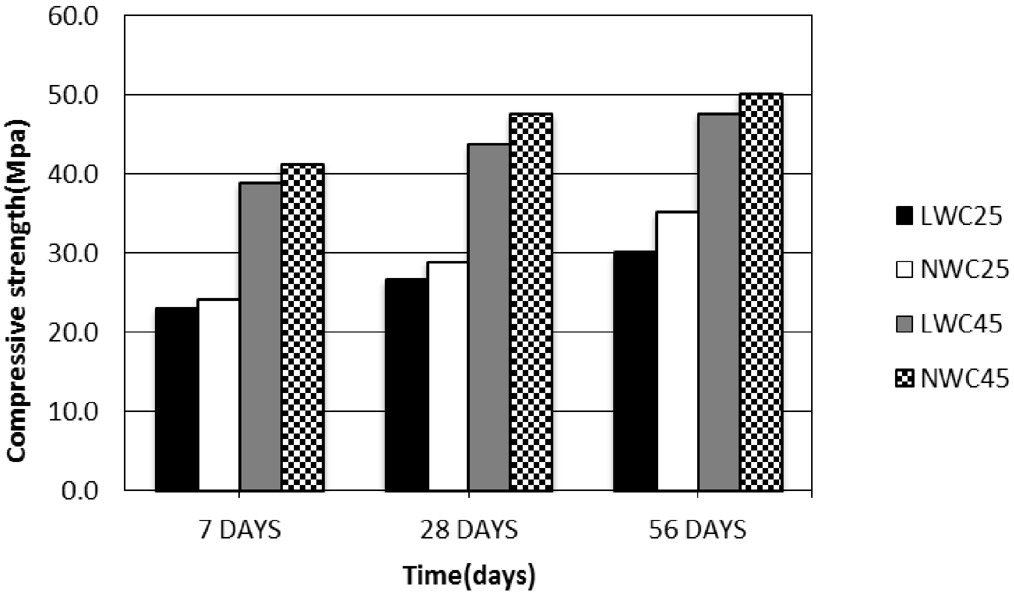

Figure 4.1 Compressive strength under various ages

4.2. Water Permeability

The size and continuity of the pores at any point during the hydration process would control the permeability coefficient [42, 50]. The permeability of concrete plays an important role in durability as it controls the rate of entry of moisture that may contain aggressive chemicals and the movement of water [82]. The permeability is adversely affected by its age, this is attributed to the completion of the hydration process which leads to the increase in the volume of gel and hydration products and hence decreases the voids [51]. Water permeability of two types of concretes was measured at 28 and 56 days and the results were shown in Table 4.2 and Figure 4.2. It can be noted in Figure 4.2 that the water ingress through LWC25 and LWC45 concretes were 18.8 and 13.5 mm at 28 days, respectively, and 13.5 and 8.5 mm at 56 days, respectively. NWC25 and NWC45 concretes, however, had water penetration of 17.6 and 11.8 mm at 28 days, and 12 and 6 mm at 56 days, respectively. This indicates 11 and 29 % increase in the water permeability of the

56-day cured concretes as the lightweight coarse aggregates has been used. Moreover, there was a substantial decrease in the water depth penetrated into the concretes with the prolonged curing, irrespective of the concrete type. However, this effect appeared to be more pronounced in NWC than in LWC such that the reduction in the water penetration from 28 to 56 days was about 31 and 49 % for the low and high strength NWCs, respectively, while the former and the latter being about 28 and 37 % in the case of LWCs. A similar result was reported by Nyame [83] in that the mortars including lightweight sand were about twice as permeable as those prepared with natural sand. In the study of Chia and Zhang [61], permeability of NWC was found to be greater or near to each other than those of LWC made with expanded clay.

Table 4.2 Water permeability values of NWC and LWC

Water Permeability Test	**28 days**	**56 days**
Code No.	**Depth of Water (mm)**	**Depth of Water (mm)**
LWC25	18.8	13.5
NWC25	17.6	12
LWC45	13.5	8.5
NWC45	11.8	6

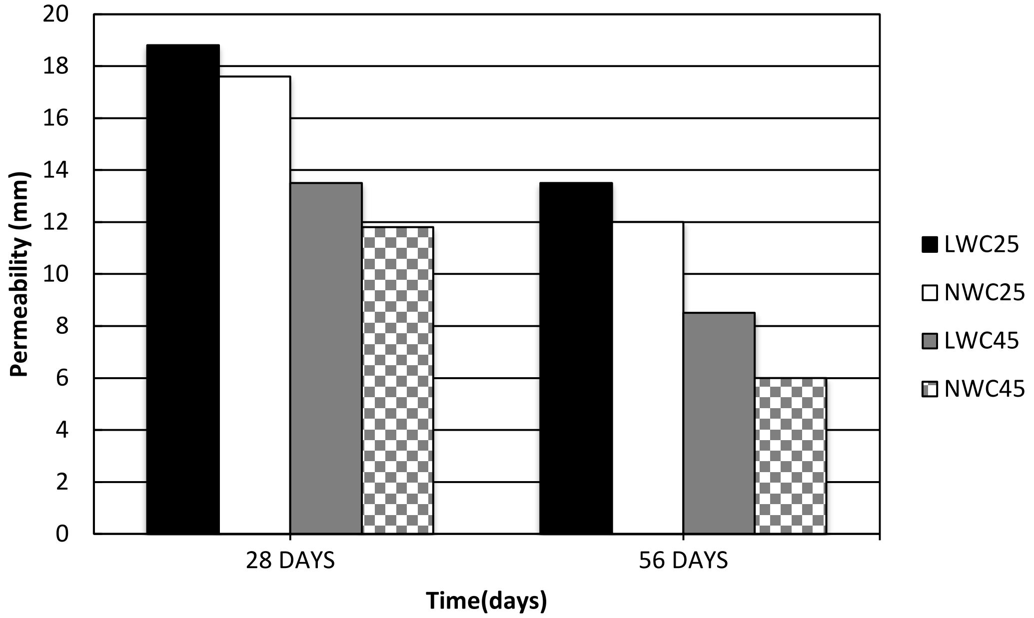

Figure 4.2 Water permeability under various ages

4.3. Chloride Ion Permeability

Table 4.3 and Figure 4.3 demonstrate the resistance of the concretes to chloride-ion penetration. Irrespective of the design compressive strength, LWC seemed to have higher total charge passed (total coulombs) compared to that of NWC, indicating that the former being less resistant against the chloride ion ingress. The charges passed through NWCs were all within the range of 2000 to 4000 coulombs (C) so as to be classified as ‘‘moderate” chloride penetrability according to AASHTO T277 [78] except for the mixture NWC25 at 28 days which had a high rating of chloride ion ingress. However, as the lightweight coarse aggregate was used, the concretes became more permeable as seen in Figure 4.3. Both normal and high strength LWCs tested at 28 days were of high ratings owing to the chloride ion permeability of as high as 6608 C and 4845 C, respectively. Only LWC45 had a total charge passed of 3146 C, leading to have moderate classification. In the study of Al-Khaiat and

Haque [13] concentration of chloride penetrated into the LWC were slightly higher than that in NWC of the same 28 days designed compressive strength of 50 MPa. This finding may be attributed to the rather high porous microstructure of cold bonded fly ash aggregates.

Table 4.3 RCPT values of NWC and LWC

Chloride Ion Permeability	**28 days**	**56 days**
Code No.	**Charge passed C**	**Charge passed C**
LWC25	6608.2	4906.7
NWC25	4791.6	3476
LWC45	4845.7	3146
NWC45	3599	2839.1

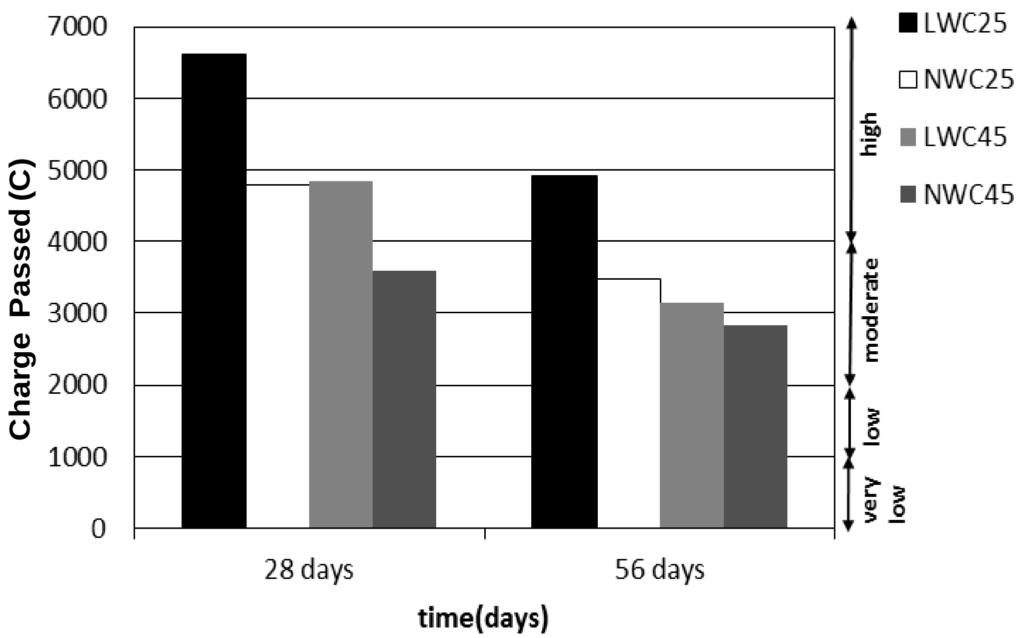

Figure 4.3 Chloride ion permeability under various ages

4.4. Gas Permeability

Apparent gas permeability of each concrete has been calculated according to Eqn. 1 using the volumetric gas flow rate obtained at the end of the 10 min interval at each stress level. RILEM TC 116 [79] recommends the use of 150, 200 and 300 kPa inlet pressures for determination of the average gas permeability coefficient. Thus, the coefficients of apparent gas permeability determined according to RILEM on the concrete specimens are presented in Table 4.4 and Figure 4.4. It was observed that permeability coefficients were found to be 3.11-5.32 ($x10^{-16}$) m^2 for LWCs and 1.62-4.13 ($x10^{-16}$) m^2 for NWCs, irrespective of the testing age and w/c ratio. Test results exhibited lower gas permeability of NWCs compared to those of LWCs, especially at low w/c ratio. For instance, for the design strength of 45 MPa, NWCs had gas permeability of as low as 78 and 91% at 28 and 56 days, respectively according to the companion LWCs. This effect appeared to be much less for the design strength of 25 MPa. This is attributed to that a concrete with a low porosity is never completely inaccessible to gases and with higher porosity gases can penetrate the concrete more easily [47]. Moreover, porous structure of cold-bonded fly aggregates contributes to the permeability of matrix, thus leading to high permeability. A similar finding was reported in the study of Sugiyama et al.[66] in that for the same w/c ratios of 0.4 and 0.6, the gas permeability of NWC was apparently lower than that of LWC made with expanded shale.

Table 4.4 Gas permeability values of NWC and LWC

Pressure Level (KPa)	GAS PERMEABILITY (m^2)							
	LWC25		LWC45		NWC25		NWC45	
	28 days	56 days	28 days	56 days	28 days	56 days	28 days	56 days
150	**7.92374E-16**	**5.40E-16**	**4.46E-16**	**3.29E-16**	**5.44286E-16**	**4.25E-16**	**2.69258E-16**	**1.96E-16**
200	**4.76846E-16**	**4.50E-16**	**3.35979E-16**	**3.18E-16**	**4.50E-16**	**3.97E-16**	**1.75E-16**	**1.67E-16**
250	3.92278E-16	3.97E-16	2.75588E-16	3.14E-16	2.75588E-16	3.73E-16	1.6623E-16	1.41E-16
300	**3.27695E-16**	**3.48E-16**	**2.44649E-16**	**2.85E-16**	**2.44649E-16**	**3.36E-16**	**1.32269E-16**	**1.24E-16**
350	3.26688E-16	2.78E-16	2.37939E-16	2.54E-16	2.37939E-16	3.19E-16	1.18274E-16	1.11E-16
400	3.09128E-16	2.73E-16	2.38125E-16	2.74E-16	2.38125E-16	3.03E-16	1.15193E-16	1.28E-16
450	2.91062E-16	2.60E-16	2.67E-16	2.33E-16	2.67E-16	2.72E-16	1.14414E-16	1.14E-16
500	2.93077E-16	2.69E-16	2.80E-16	2.17E-16	3.50E-16	2.51E-16	1.47703E-16	1.33E-16
Mean	**5.32305E-16**	**4.46215E-16**	**3.42281E-16**	**3.10643E-16**	**4.1312E-16**	**3.85729E-16**	**1.92206E-16**	**1.62441E-16**

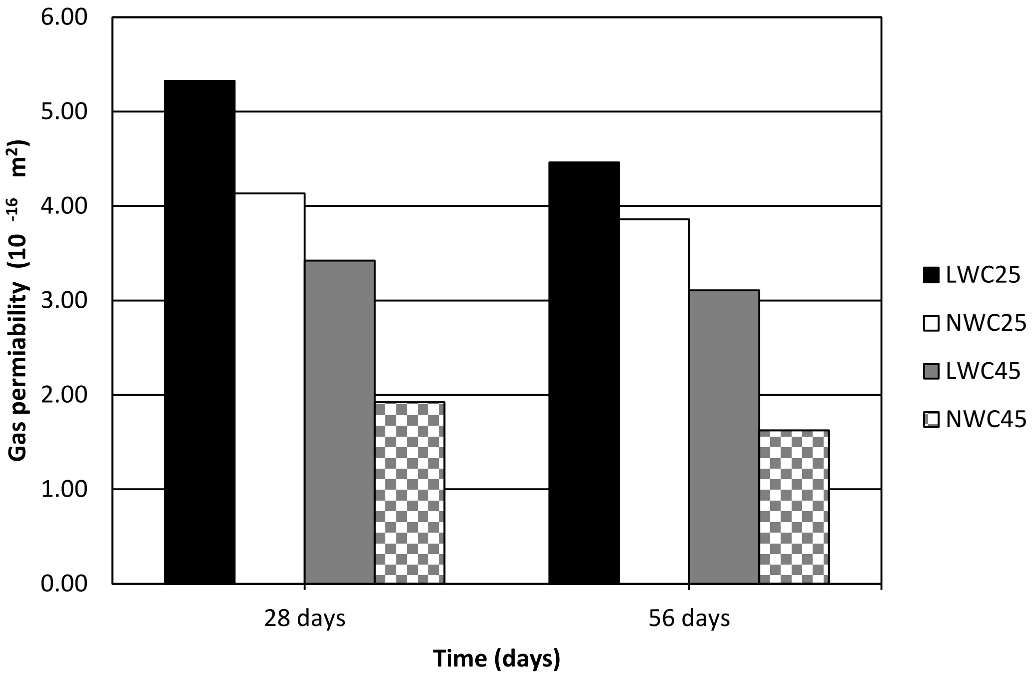

Figure 4.4 Gas permeability under various ages

4.5. Sorptivity Index

The value of sorptivity illustrates the water mass uptake by concrete from the bottom surface based on water flowing into the concrete through large connected pores [62, 81]. The change in sorptivity with concrete age for the NWC and LWC are given in Table 4.5 and Figure 4.5 and it can be noted that the sorptivity through LWC25 and LWC45 concretes were 0.304 and 0.198 $mm/min^{1/2}$ at 28 days respectively, and 0.223 and 0.141 $mm/min^{1/2}$ at 56 days, respectively. As seen in gas permeability, however, NWC25 and NWC45 concretes had almost 43 and 45% lower sorptivity than those of LWCs, for a given curing period of 56 days. The reason for this lies in the higher porosity of lightweight aggregates which in turn helped in increasing the sorptivity of LWCs. According to Lie et al. [60] NWC had higher water sorptivity by a ratio of 1.1 than LWC while the former had lower sorptivity value than another corresponding LWC by a ratio of 3 indicating that the sorptivity of LWCs was greatly influenced by the lightweight aggregate type.

Table 4.5 Sorptivity values of NWC and LWC

Sorptivity	**28 days**	**56 days**
Code No.	**mm/min$^{1/2}$**	**mm/min$^{1/2}$**
LWC25	0.304	0.223
NWC25	0.161	0.126
LWC45	0.198	0.141
NWC45	0.123	0.076

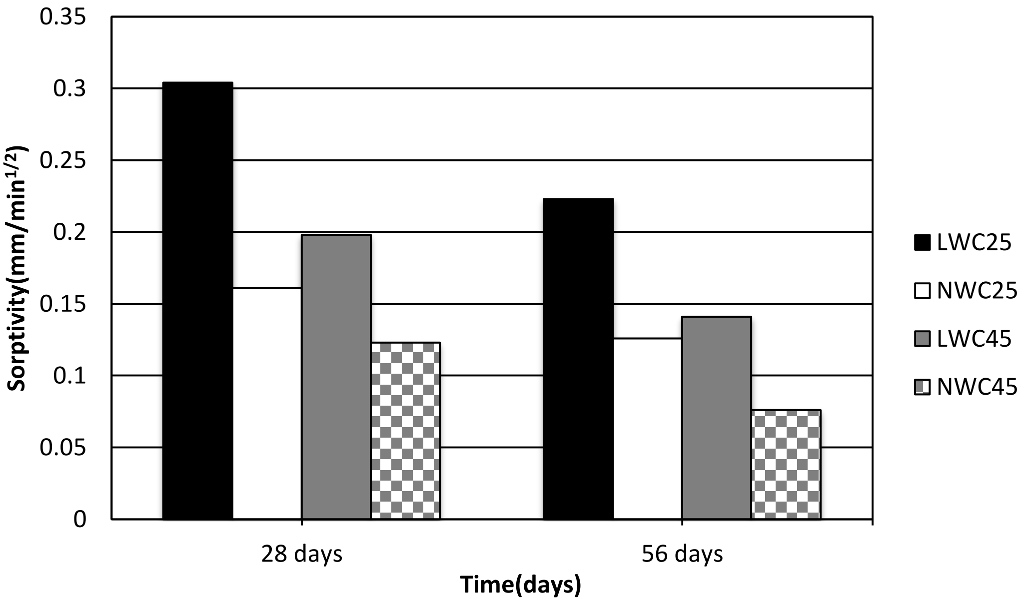

Figure 4.5 Sorptivity under various ages

4.6. Relations and Correlations between Compressive Strength and Transport Properties

1. Water Permeability: Variation of water permeability with the compressive strength of the concretes is presented in Figure 4.6. It was observed that, a power law regression fit of the data of both NWC and LWC yielded a good correlation with a correlation coefficient of 0.74 and 0.70, respectively. The rate of reduction in the water permeability of the concretes was almost similar as seen in Figure 4.6.

2. Chloride Penetration: The influence of curing period and compressive strength were to decrease the chloride ion ingress of both concretes in the same way. It was noted in Figure 4.7 that, however, the rate of decrease in the chloride ion ingress seemed to be steeper for LWCs.

3. Gas Permeability: Figure 4.8 exhibits the variation of gas permeability with compressive strength of the concretes. It was evident that the strength increase made the concretes more resistant to ingress of fluids and gases, especially in the case of NWCs. Indeed, gas permeability of the concretes decreased more than 30 and 50 % for LWC and NWC, respectively, as the design strength increased from 25 to 45 MPa.

4. Sorptivity: There was a good correlation between the compressive strength and the sorptivity, irrespective of the concrete type. As seen in Figure 4.9, higher the compressive strength, lower the sorptivity for both LWC and NWC.

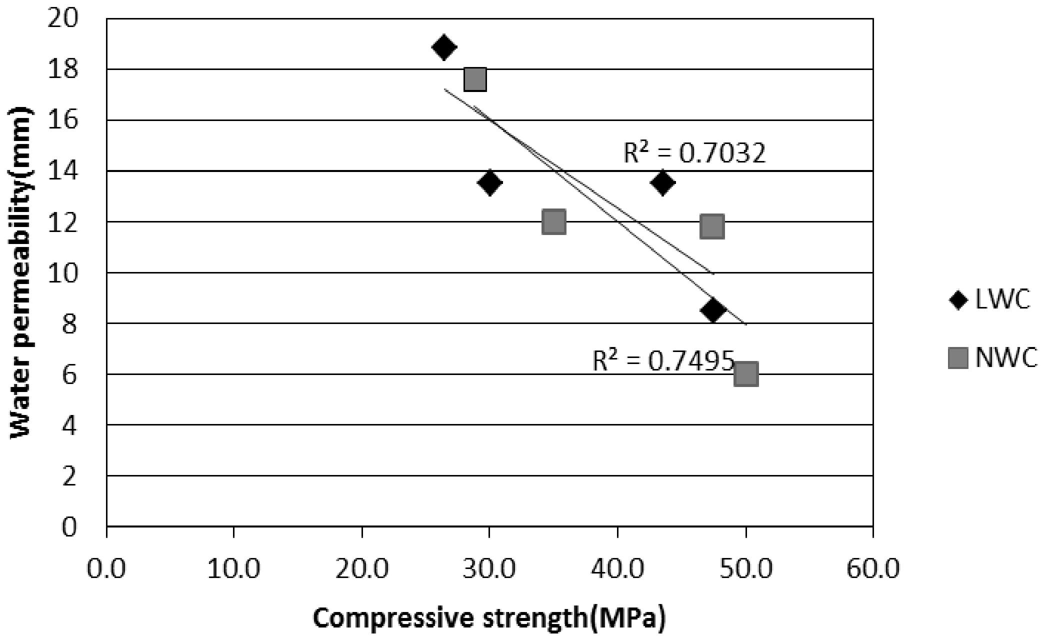

Figure 4.6 Relationship between compressive strength and water permeability under various ages

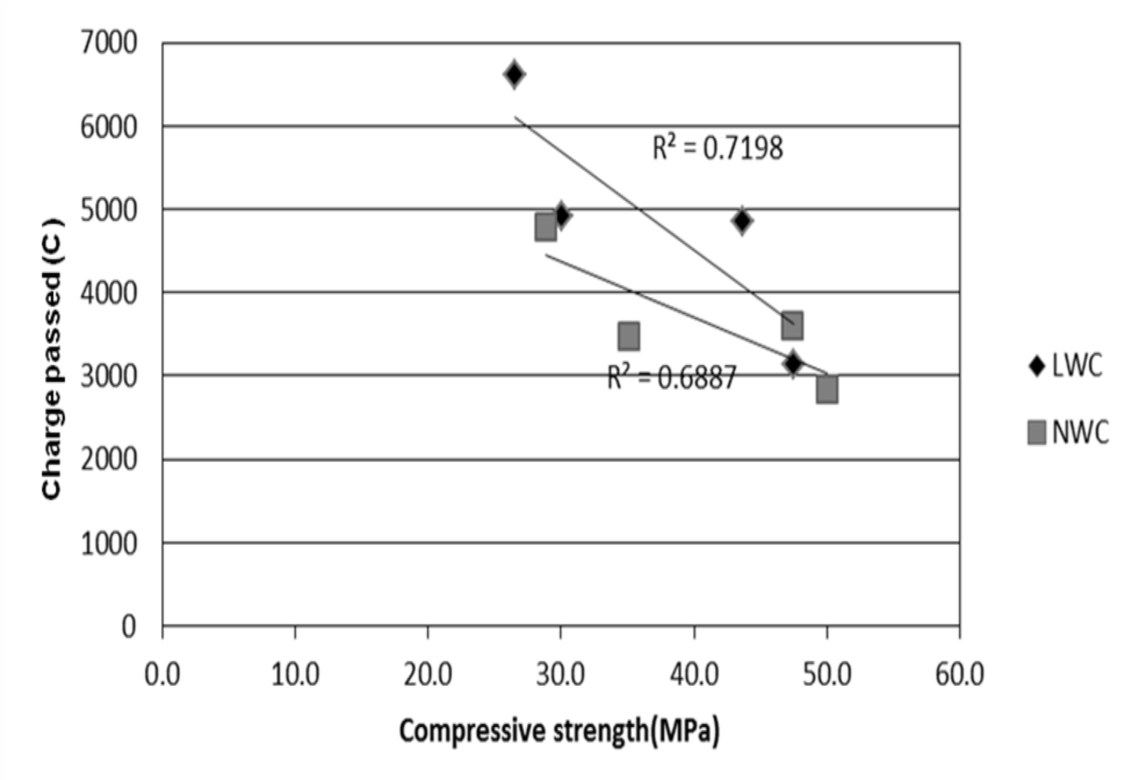

Figure 4.7 Relationship between compressive strength and Chloride Penetration under various ages

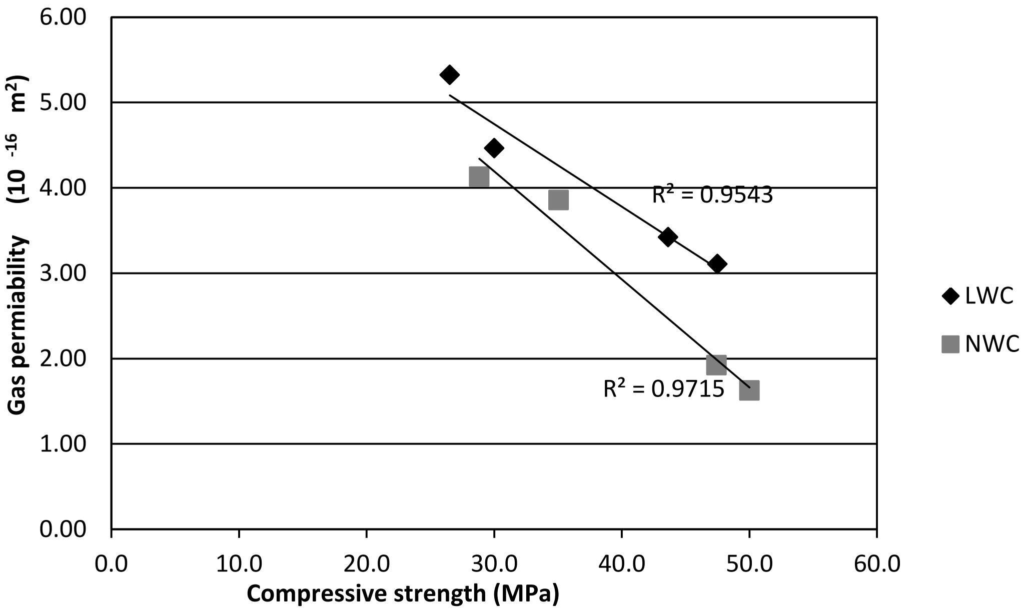

Figure 4.8 Relationship between compressive strength and gas permeability under various ages

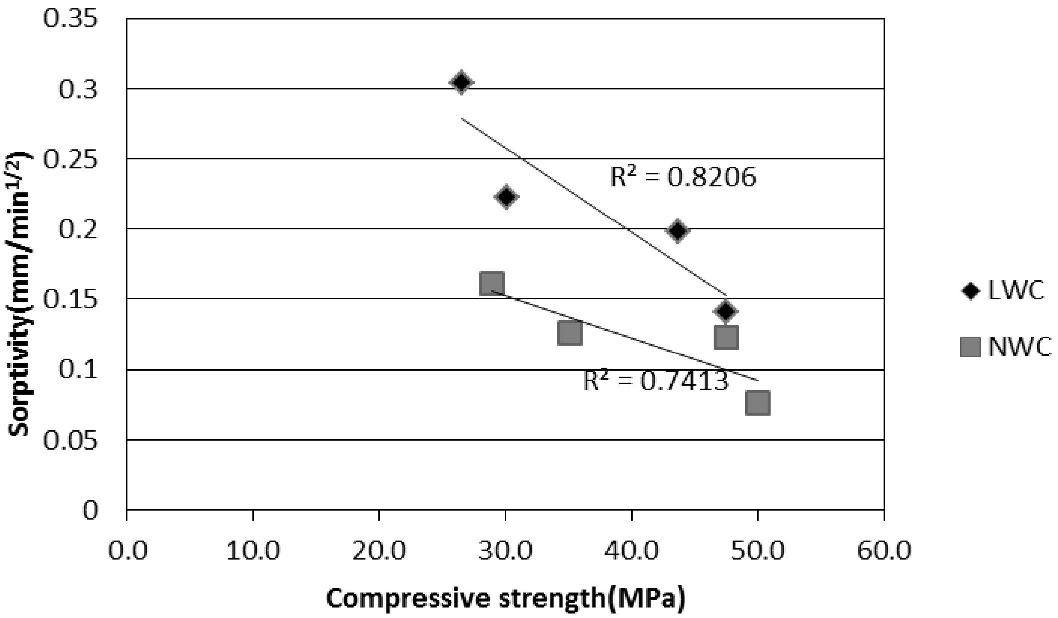

Figure 4.9 Relationship between compressive strength and sorptivity under various ages

CHAPTER 5

CONCLUSIONS

Based on the findings of the experimental program presented above, the following conclusions may be drawn:

- For the similar design strength, LWCs had lower compressive strengths than NWCs by about 14%. Lowering the w/c ratio enhanced the compressive strength for both LWCs and NWCs. However, this beneficial effect was less for LWCs since the further improvement of the matrix did not necessarily mean higher compressive strength for concrete due to the earlier failure of the lightweight coarse aggregate particles.
- Developing the compressive strength accompanied by decreasing each of water permeability, chloride ion permeability, gas permeability, and sorptivity for both LWC and NWC can be concluded. This correlation was generally close to each other or better for LWC than NWC, especially for chloride ion permeability and sorptivity.
- LWC with cold-bonded fly ash appeared to have poor transport properties than corresponding NWC, especially in terms of water permeability. The reason for this lies in the higher porosity of lightweight aggregates which in turn helped in increasing the permeability of LWCs.
- Lightweight aggregates may be used in LWC to achieve lower unit weight and stop using natural aggregates; however reduced resistance to chloride-ion penetration as well as high water and gas permeability of LWCs with lightweight aggregates should be taken into consideration.

- This investigation may be considered as an environmental friendly research or green research because it will really treat a part of environmental issues by using disposal material like fly ash through an easy process which consumes a minimum energy. Just in Turkey more than 15 million tons out of 600 million tons produced in the world, from thermal coal-fired power plants and up to the time of now only a very little proportion of it is used in the building industry and other different purposes.

REFERENCES

[1] Haque M.N., Al-Khaiat H., and Kayali O. (2004). Strength and durability of lightweight concrete. *Cement and Concrete Composites*, 26, pp. 307–314

[2] Newman, J.B. and Bremner, T.W. (1980). The testing of Structural Lightweight Concrete. The Concrete Society, The Construction Press, Lancaster, UK, pp. 152– 172.

[3] Zhang, M.H. and Gjorv, O.E. (1991). Mechanical properties of high strength lightweight concrete. *ACI Material Journal*, V. 88, No. 3, pp. 240–247

[4] Lo, Y., GAO, X.F., and Jeary, A.P. (1999). Microstructure of pre-wetted aggregate on lightweight concrete. *Building and Environment*, V. 34, pp. 759-764

[5] Bilodeau, A. and Malhotra, V.M. (2000). High-volume fly ash system: Concrete solution for sustainable development. *ACI Material Journal,* V.97, No. 1, pp. 41–49.

[6] Yun, B., Ratiyah, I., and Basheer, P.A.M. (2004). Properties of lightweight concrete manufactured with fly ash, furnace bottom ash, and Lytag. International workshop on sustainable development and concrete technology, Beijing. p. 77–88

[7] Kayali, O., Haque, M.N., and Zhu, B. (1999). Drying shrinkage of fiber-reinforced lightweight aggregate concrete containing fly ash. *Cement and Concrete Research*, V.29,pp 1835–1840

[8] Chi, J.M., Huang, R., Yang, C.C., and Yang, J.J. (2003) Effect of aggregate properties on the strength and stiffness of the lightweight concrete. *Cement and Concrete Composites,* V.25, pp. 197–205

[9] Chang, T.P. and Shieh, M.M. (1996) Fracture properties of lightweight concrete, *Cement and Concrete Research*, V. 26, No. 2, pp. 181– 188

[10] Yang, C.C. (1997). Approximate elastic moduli of lightweight aggregate. *Cement and Concrete Research*, V.27, No. 7, pp. 1021– 1030.

[11] Gesoglu, M., Ozturan, T., and Guneyisi, E. (2004). Shrinkage cracking of lightweight concrete made with cold-bonded fly ash aggregates. *Cement and Concrete Research*, V.34, No.7, pp. 1121–1130

[12] Torres, M.L. and Garcia-Ruiz, P.A. (2009). Lightweight pozzolanic materials used in mortars: Evaluation of their influence on density, mechanical strength and water absorption. *Cement and Concrete Composites*, V.31, pp. 114–119

[13] Al-Khaiat, H. and Haque, N. (1999). Strength and durability of lightweight and normal weight concrete. *ASCE Journal Material Civil Eng*., V.11, No.3, pp.231–235

[14] Ke, Y., Beaucour, A.L., Ortola, S., Dumontet, H., and Cabrillac, R. (2009). Influence of volume fraction and characteristics of lightweight aggregates on the mechanical properties of concrete. *Construction Building Material*, V. 23, pp. 2821–2828

[15] Khokhrin, N.K. (2009). Durability of Lightweight Concrete Structure Members. (Kuibyshov, U.S.S.R.).

[16] Thomas, M.D.A. (2006). Chloride diffusion in high-performance lightweight aggregate concrete. In: Durability of concrete. proceedings 7th CANMET/ACI international conference, SP234, Montreal, Canada. p. 77–95

[17] U.S. Department of Transportation, Federal Highway Administration Fly Ash Facts for Highway Engineers"

[18] American Coal Ash Association www.acaa-usa.org

[19] Erdogan ö. (2007). Effects of mineral admixtures on the fresh and hardened properties of self compacting concretes: binary, ternary and quaternary systems. PhD thesis. Gaziantep University.

[20] Doven AG (1996) Lightweight fly ash aggregate production using cold bonding agglomeration process. Ph. D. Thesis, Boğaziçi University, Turkey

[21] Human and Ecological Risk. (2007). Assessment of Coal Combustion Wastes, RTI, Research Triangle Park, prepared for the U.S. Environmental Protection Agency

[22] ASTM C618 – 08. Standard Specification for Coal Fly Ash and Raw or Calcined Natural Pozzolan for Use in Concrete". *ASTM International*

[23] AASHTO M 295. (2011). Standard Specification for Coal Fly Ash and Raw or Calcined Natural Pozzolan for Use in Concrete

[24] Myers, J. F., K. (1976). Pichumani and S. Bernadette Fly Ash-A Highway Construction Material. U.S. Department of Transportation, FHWA-IP-76-16, Monroeville, Pennsylvania.

[25] U.S. Federal Highway Administration. "Fly Ash Facts for Highway Engineers"

[26] American Coal Ash Association (ACAA). (2006). coal combustion product (CCP) production and use. Aurora, CO: *American Coal Ash Association*; August, (2007).

[27] Federal Highway Administration (FHWA). (2003). American Coal Ash Association (ACAA). Fly ash facts for highway engineers. Federal Highway Administration (FHWA), FHWA-IF-03-019.

[28] Gonzalez-Corrochano B., Alonso-Azcarate J. and Rodas M. (2009). Production of lightweight aggregates from mining and industrial wastes. *Journal of Environmental Management,* 90.2801–2812.

[29] Venuat M. (2005). Lightweight Aggregates-An Updating Survey of Materials, Production Technology, Innovations and Inventions. Centre d'etudes et de Recherches de L'industrie des Liant Hydrouliques, France

[30] Topcu I.B. and Uygunoglu T. (2007). Properties of autoclaved lightweight aggregate concrete. *Building and Environment,* 42 4108–4116.

[31] Clinker from Wikipedia, the free encyclopedia.

[32] Portland cements Association Sustainable Manufacturing Fact Sheet. IRON AND STEEL BYPRODUCTS"

[33] Benjamin L. Phillips, Jack Groppo, and Roger Perrone. Evaluation of Processed Bottom Ash for Use as Lightweight Aggregate in the Production of Concrete Masonry Units." 2540 Research Park Drive. Lexington, KY 40511-8410

[34] http://www.vijayacement.com/fly-ash.html

[35] Structural light weight concrete. (1993). By John L. Clarke, first edition.

[36] Ramadan KZ. (1995). Composite and aggregate production using high calcium fly ash. PhD thesis. Istanbul, Boğaziçi University.

[37] Basic facts about perlite, http://www.perlite.net

[38] http://rruff.geo.arizona.edu/doclib/hom/vermiculite.pdf Handbook of Mineralogy, http://www.mindat.org/min-4170.html

[39] Gesoglu M. (2004). Effects of lightweight aggregate properties on mechanical, fracture, and physical behavior of lightweight concretes. PhD thesis. Istanbul, Boğaziçi University.

[40] Jaroslav, S. and Z. Ruzickova. (1987). Pelletization of Fines, Ore Research Instituted-Prague, Elsevier Science Publishing Company, New York.

[41] Pietsch, W. (1991). Size Enlargement by Agglomeration, New York: John Wiley and Sons.

[42] Neville AM. (1995). Properties of concrete. Burnt Mill, Harlow, Essex, New York: Longman.

[43] Broomfield JP. (1997). Corrosion of steel in concrete: understanding, investigation and repair. London (UK): E&FN Spon Ltd.

[44] B. B. Sabir, S. Wild and M. O'Farrell. (1998). Materials and Structures, A water sorptivity test for mortar and concrete Vol. 31, pp. 568-574.

[45] W.J. McCarter, M. Forde, H.W. Whittington, T. Simons. (1983). Electrical resistivity characteristics of air-entrained concrete, Proc. Inst. Civ. Eng. Pt. 2 75 123–127.

[46] H.S. Wong, A.M. Pappas, R.W. Zimmerman. (2011). Effect of entrained air voids on the microstructure and mass transport properties of concrete , N.R. Buenfeld , *Cement and Concrete Research,* 41 1067–1077

[47] P. Van den Heede, E. Gruyaert, N. De Belie. (2010). Transport properties of high-volume fly ash concrete: Capillary water sorption, water sorption under vacuum and gas permeability, *Cement & Concrete Composites,* 32 749–756.

[48] Aligizaki KK. (2006). Pore structure of cement-based materials: testing, interpretation and requirements. Taylor & Francis.

[49] C.C. Yang, C.H. Liang. (2009). the influence of medium–high temperature on the transport properties of concrete by using accelerated chloride migration test, Materials Chemistry and Physics 114 670–675.

[50] Mehta PK, Monteiro PJM. (1993). concrete: structure, properties and materials. 2nd ed. Prentice Hall.

[51] C.M. Tam, Vivian W.Y. Tam, K.M. Ng. (2012).Assessing drying shrinkage and water permeability of reactive powder concrete produced in Hong Kong. Construction and Building Materials 26 79–89

[52] J. Wongpa, K. Kiattikomol, C. Jaturapitakkul, P. Chindaprasirt. (2010). Compressive strength, modulus of elasticity, and water permeability of inorganic polymer concrete.Materials and Design 31 4748–4754

[53] Sang-Soon Park, Seung-Jun Kwon, Sang hwa Jung, Sang-Woong Lee. (2011). Modeling of water permeability in early aged concrete with cracks based on micro pore tructure. Construction and Building Materials doi:10.1016/j.conbuildmat.2011.07.002

[54] P. Chindaprasirt, S. Homwuttiwong, C. Jaturapitakkul. (2007). Strength and water permeability of concrete containing palm oil fuel ash and rice husk–bark ash. *Construction and Building Materials*, 21 1492–1499

[55] Weerachart Tangchirapat, Chai Jaturapitakkul. (2010). Strength, drying shrinkage, and water permeability of concrete incorporating ground palm oil fuel ash. *Cement & Concrete Composites*, 32 767–774

[56] Seong-Tae Yi, Tae-Yang Hyun, Jin-Keun Kim. (2011). the effects of hydraulic pressure and crack width on water permeability of penetration crack-induced concrete. *Construction and Building Materials*, 25 2576–2583

[57] P. Mohr, W. Hansen, E. Jensen, I. Pane. (2000). Transport properties of concrete pavements with excellent long-term in-service performance. *Cement and Concrete Research*, 30 1903-1910

[58] Amarnath Yerramala, K. Ganesh Babu. (2011). Transport properties of high volume fly ash roller compacted concrete. Cement & Concrete Composites doi:10.1016/j. *Cement and Concrete,*.2011.07.010.

[59] Mohammed Sonebi and Sreejith Nanukuttan. (2009). Transport Properties of Self-Consolidating Concrete. *ACI Materials Journal*, V. 106, No. 2.

[60] Xuemei Liu, Kok Seng Chia, Min-Hong Zhang. (2011). Water absorption, permeability, and resistance to chloride-ion penetration of lightweight aggregate concrete. *Construction and Building Materials*, 25 335–343

[61] Kok Seng Chia, Min-Hong Zhang. (2002). Water permeability and chloride penetrability of high-strength lightweight aggregate concrete. *Cement and Concrete Research,* 32 639–645

[62] Erhan Güneyisi, Mehmet Gesoglu, and Erdogan Özbay. (2011). Permeation Properties of Self-Consolidating Concretes with Mineral Admixtures. *ACI Materials Journal*, V. 108, No. 2.

[63] ASTM C 1202-94. (1995). Standard method for electrical indication of concretes ability of resist chloride ion penetration. Annual book of ASTM standards, vol. 4.02. p. 624–9

[64] Sabine Care, François Derkx. (2011). Determination of relevant parameters influencing gas permeability of mortars. *Construction and Building Materials*, 25 1248–1256

[65] Vincent Picandet, Abdelhafid Khelidj, Guy Bastian. (2001). Effect of axial compressive damage on gas permeability of ordinary and high-performance concrete .*Cement and Concrete Research*, 31 1525–1532

[66] Takafumi Sugiyama, Theodore W. Bremner, and Thomas A. Holm. (1996). Effect of Stress on Gas Permeability in Concrete. *ACI Materials Journal*, V. 93, No. 5.

[67] Shi Hui-sheng, Xu Bi-wan, Zhou Xiao-chen. (2009). Influence of mineral admixtures on compressive strength, gas permeability and carbonation of high performance concrete. *Construction and Building Materials,* 23.

[68] S. Tsivilis, E. Chaniotakisb, G. Batis, C. Meletioub, V. Kasselouria, G. Kakali, A. Sakellariou, G. Pavlakis, C. Psimadas. (1999). the effect of clinker and limestone quality on the gas permeability, water absorption and pore structure of limestone cement concrete. *Cement and Concrete Composites*, 21 139-146

[69] Erhan Guneyisi and Kasım Mermerdas. (2007). Comparative study on strength, sorptivity, and chloride ingress characteristics of air-cured and water-cured concretes modified with metakaolin. *Materials and Structures,* 40 1161–1171

[70] J. Bai, S. Wild, B.B. Sabir. (2002). Sorptivity and strength of air-cured and water-cured PC–PFA–MK concrete and the influence of binder composition on carbonation depth. *Cement and Concrete Research*, 32 1813–1821

[71] Turkish Standard TS EN 197-1. (2002). Çimento- bölüm 1: genel çimentolar- bileşim, özellikler ve uygunluk kriterleri.

[72] ASTM C 127. (2007). Standard test method for specific gravity and absorption of coarse aggregate, Annual Book of ASTM Standards.

[73] BS 812, part 110: (1990) Methods for determination of aggregate crushing value (ACV).

[74] BS EN 12350-2Testing fresh concrete. Slump test. This replaces BS 1881: Part 102.

[75] ASTM C192Standard Practice for Making and Curing Concrete Test Specimens in the Laboratory”

[76] ASTM C 39. (2010). Standard test method for compressive strength of cylindrical concrete specimens. Annual Book of ASTM Standards.

[77] TS EN 12390-8. (2002). Testing Hardened Concrete—Part 8: Depth of Penetration of Water under Pressure. Institute of Turkish Standards, Ankara, Turkey.

[78] AASHTO T277.Standard Method of Test for Rapid Determination of the Chloride Permeability of Concrete”

[79] RILEM TC 116-PCD. (1999). Permeability of concrete as a criteron of its durability. *Materials and Structures*, 32, pp.174-179

[80] ASTM C 1585.Standard Test Method for Measurement of Rate of Absorption of Water by Hydraulic-Cement Concretes”

[81] Abdul Razak, H., Chai, H.K., and Wong, H.S. (2004). Near surface characteristics of concrete containing supplementary cementing materials. *Cement and Concrete Composites*, V.26,pp. 883–889

[82] Mindess S, Young F, Darwin D. (2003). Concrete. Upper Saddle River. NJ: Prentice Hall.

[83] Nyame, B.K. (1986). Permeability of normal and lightweight mortars. *Magazine of Concrete Research*, V.38, No. 134.

APPENDIX A. PHOTOGRAPHIC VIEWS

(a)

(b)

(c)

(d)

(e)

(f)

Figure A1 Photographic view of LWA creation by cold bonding process a) 1st minute, b) 3rd minute, c) 9th minute, d) 11th minute, e) 15th minute, f) 18th and last minute.

Figure A2 Photographic view of working during production of LWA

Figure A3 Photographic view of dried LWA in an oven

Figure A4 Photographic view of weighted LWA for calculation water absorption